Pluripotency of hiPS cells after liquid nitrogen preservation

In vitro histochemical analysis of hiPS cells after preservation in liquid nitrogen

After thawing and 4 days of culture, cells were fixed in 4% (w/v) paraformaldehyde (PFA) in PBS for 15 min and permeabilized by treatment with 0.2% (v/v) Triton X-100 solution for 15 min at RT. After treatment with the Blocking One® reagent (Nacalai Tesque) at RT for 1 h, cells were incubated with primary antibodies for 12 h at 4°C. The dilution ratios of the primary antibodies were as follows: mouse anti-SSEA-4, 1:400 (Chemicon, CA), and rabbit anti-Oct3/4, 1:200 (Santa Cruz Biotechnology, CA) (diluted in Blocking One® solution). The sample cells were washed in 0.05% (w/v) polyoxyethylene sorbitan monolaurate (Tween 20, in PBS, Wako) three times and then incubated with secondary antibodies for 2 h at RT. The dilution ratios of the secondary antibodies were as follows: Alexa Fluor® 488-labeled goat anti-mouse IgG, 1:500 (Invitrogen), and Alexa Fluor® 594-labeled goat anti-rabbit IgG, 1:500 (Invitrogen) (diluted in Blocking One® solution). To stain cell nuclei, the sample cells were incubated with Hoechst 33342 fluorescent dye (Dojindo Laboratories, Kumamoto, Japan) at a dilution of 1:500 in PBS for 15 min at RT. After washing with PBS, the sample cells were observed under a fluorescent microscope (IX71, Olympus Optical Co. Ltd., Tokyo, Japan). The alkaline phosphatase activity of the hiPS cells was visualized after fixation with PFA using the Alkaline Phosphatase Substrate Kit III (Vector Laboratories, Burlingame, CA, USA).

Teratoma formation by hiPS cells after preservation in liquid nitrogen using VS2E

hiPS cells were preserved under liquid nitrogen using VS2E and cultured for 1 passage. Cells were treated with 10 μM Y-27632 (Wako) for 1 h at 37°C before collection from the 100-mm culture dishes. Cells from a single dish were subcutaneously injected into the backs (right and left sides) of SCID mice. After 12 weeks, teratomas were removed and fixed in 4% (w/v) PFA solution overnight. Paraffin-embedded tissue sections (4 μm) were prepared using standard methods and stained with hematoxylin and eosin (HE) for visual examination.

Statistical analysis

Comparisons between two groups were made using Student's *t*-tests, and $p < 0.05$ was considered statistically significant. All statistical calculations were performed using statistical software (JMP 6.0).

Acknowledgements

This study was supported in part by a Grant-in-Aid for Scientific Research (A) (No. 21240051), by a Challenging Exploratory Research Grant (No. 21650118) from the Ministry of Education, Culture, Sports, Science, and Technology (MEXT) of Japan, and by the Ministry of Health, Labor, and Welfare of Japan (H20-007).

References

AGUDELO, C.A., and IWATA, H. (2008). The development of alternative vitrification solutions for microencapsulated islets. *Biomaterials* 29: 1167-1176.

AGUDELO, C.A., TERAMURA, Y., and IWATA, H. (2009). Cryopreserved agarose-encapsulated islets as bioartificial pancreas: a feasibility study. *Transplantation* 87: 29-34.

AMEEN, C., STREHL, R., BJORQUIST, P., LINDAHL, A., HYLLNER, J., and SARTIPY, P. (2008). Human embryonic stem cells: Current technologies and emerging industrial applications. *Crit. Rev. Oncol. Hematol.* 65: 54-80.

CHUNG, M., LOWE, R.D., CHAN, Y.H.M., GANESAN P.V., and BOXER, S.G. (2009). DNA-tethered membranes formed by giant vesicle rupture. *J. Struct. Biol.* 168: 190-199

GLAASSEN, D.A., DESLER, M.M., and RIZZINO, A. (2009). ROCK inhibition enhances the recovery and growth of cryopreserved human embryonic stem cells and human induced pluripotent stem cells. *Mol. Reprod. Dev.* 76: 722-732.

FUJIOKA, T., YASUCHIKA, K., NAKAMURA, Y., NAKATSUJI, N., and SUEMORI, H. (2004). A simple and efficient cryopreservation method for primate embryonic stem cells. *Int. J. Dev. Biol.* 48: 1149-1154.

GREEN, R.J., DAVIES, J., DAVIES, M.C., ROBERTS, C.J., and TENDLER S.J. (1997). Surface plasmon resonance for real time *in situ* analysis of protein adsorption to polymer surfaces. *Biomaterials* 18: 405-413.

HIRATA, I., MORIMOTO, Y., MURAKAMI, Y., IWATA, H., KITANO, E., and KITAMURA, H. (2000). Study of complement activation on well-defined surfaces using surface plasmon resonance. *Colloids Surf. B* 18: 285–292.

JI, L., de PABLO, J., and PALECEK, S.P. (2004). Cryopreservation of adherent human embryonic stem cells. *Biotechnol. Bioeng.* 88: 299-312.

KATKOV I.I., KIM M.S., BAJPAI, R., ALTMAN, Y.S., MERCOLA, M., LORING, J.F., TERSKIKH, A.V., SNYDER, E.Y., and LEVINE, F. (2006). Cryopreservation by slow cooling with DMSO diminished production of *Oct-4* pluripotency marker in human embryonic stem cells. *Cryobiology* 53: 194-205.

KELLER, G., and SNODGRASS, H.R. (1999). Human embryonic stem cells: the future is now. *Nat. Med.* 5: 151-152.

LI, X., KRAWETZ, R., LIU, S., MENG, G., and RANCOURT, D.E. (2009). ROCK inhibitor improves survival of cryopreserved serum/feeder-free single human embryonic stem cells. *Hum. Reprod.* 24: 580-589.

MARTIN-IBAÑEZ, R., UNGER, C., STRÖMBERG, A., BAKER, D., CANALS, J.M., and HOVATTA, O. (2008). Novel cryopreservation method for dissociated human embryonic stem cells in the presence of a ROCK inhibitor. *Hum. Reprod.* 23: 2744-2754.

MOLLAMOHAMMADI, S., TAEI, A., PAKZAK, M., TOTONCHI, M., SEIFINEJAD, A., MASOUDI, N., and BAHARVAND, H. (2009). Simple and efficient cryopreservation method for feeder-free dissociated human induced pluripotent stem cells and human embryonic stem cells. *Hum. Reprod.* 24: 2468-2476.

NAKAGAWA, M., KOYANAGI, M., TANABE, K., TAKAHASHI, K., ICHISAKA, T., AOI, T., OKITA, K., MOCHIDUKI, Y., TAKIZAWA, N., and YAMANAKA, S. (2008). Generation of inducek pluripotent stem cells without Myc from mouse and human fibroblasts. *Nat. Biotechnol.* 26: 101-106.

NISHIGAKI, T., TERAMURA, Y., SUEMORI, H., and IWATA, H. (2010). Cryopreservation of primate embryonic stem cells with chemically-defined solution without Me_2SO. *Cryobiology* 60: 159-164.

PAVEY, K.D. and OLLIFF, C.J. (1999). SPR analysis of the total reduction of protein adsorption to surfaces coated with mixtures of long- and short-chain polyethylene oxide block copolymers. *Biomaterials* 20: 885-890.

REUBINOFF, B.E., PERA, M.F., VAJTA, G., and TROUSON, A.O. (2001). Effective cryopreservation of human embryonic stem cells by open pulled straw vitrification method. *Hum. Reprod.* 16: 2187-2194.

RICHARDS, M., FONG, C.Y., TAN, S., CHAN, W.K., and BONGSO, A. An efficient and safe xeno-free cryopreservation method for the storage of human embryonic stem cells. (2004). *Stem Cells* 22: 779-789.

SPERGER, J.M., CHEN, X., DRAPER, J.S., ANTOSIEWICZ, J.E., CHON, C.H. JONES, S.B., BROOKS, J.D., ANDREWS, P.W., BROWN, P.O., and THOMSON, J.A. (2003). Gene expression patterns in human embryonic stem cells and human pluripotent germ cell tumors. *Proc. Natl. Acad. Sci. USA.* 100: 13350-13355.

TAKAHASHI, K., TANABE, K., OHNUKI, M., NARITA, M., ICHISAKA, T., TOMODA, K., and YAMANAKA, S. (2007). Induction of pluripotent stem cells from adult human fibroblasts by defined factors. *Cell* 131: 861-872.

TAKAMUKU, T., TSUTSUMI, Y., MATSUGAMI, T., and YAMAGUCHI, T. (2008). Thermal Properties and Mixing State of Diol-Water Mixtures Studied by Calorimetry, Large-Angle X-Ray Scattering, and NMR Relaxation. *J. Phys. Chem. B* 112: 13300-13309

TAYLOR, J.D., PHILLIPS, K.P., and CHENG, Q. (2007). Microfluidic fabrication of addressable tethered lipid bilayer arrays and optimization using SPR with silane-derivatized nanoglassy substrates. *Lab Chip* 7: 927-930

TERAMURA, Y., CHEN, H., KAWAMOTO, T., and IWATA, H. (2010b). Control of cell attachment through polyDNA hybridization. *Biomaterials* 31: 2229-2235

TERAMURA, Y., KANEDA, Y., and IWATA, H. (2007). Islets-Encapsulation with Ultra-thin Layer-by-Layer Membranes of Poly(vinyl alcohol) through Poly(ethylene glycol)-lipids Anchored to Cell Surface. *Biomaterials,* 28, 4818-4825

TERAMURA, Y., LUAN, M.N., KAWAMOTO, T., and IWATA, H. (2010a). Microencapsulation of Islets with Living Cells Using PolyDNA-PEG-Lipid Conjugate. *Bioconjugate Chem,* 21: 792-796.

THOMAS, K.R., and CAPECCHI, M.R. (1987). Site-directed mutagenesis by gene targeting in mouse embryo-derived stem cells. *Cell* 51: 503-512.

THOMSON, J.A., KALISHMAN, L., GOLOS, T.G., DURNING, M., HARRIS, C.P., THOMSON, J.A., ITSKOVITZ-ELDOR, J., SHAPIRO, S.S., WAKNITZ, M.A., SWIERGIEL, J.J., MARSHALL, V.S. and JONES, J. (1998). Embryonic stem cell lines derived from human blastocysts. *Science* 282: 1145-1147.

YU, J., VODYANIK, M.A., SMUGA-OTTO, K., ANTOSIEWICZ-BOURGET, J., FRANE, J.L., TIAN, S., NIE, J., JONSDOTTIR, G.A., RUOTTI, V., STEWART, R., SLUKVIN, I.I., and THOMSON, J.A. (2007). Induced pluripotent stem cell lines derived from human somatic cells. *Science* 318: 1917-1920.

THE JOURNAL OF BIOLOGICAL CHEMISTRY VOL. 285, NO. 39, pp. 29842–29850, September 24, 2010

Histone Modifiers, YY1 and p300, Regulate the Expression of Cartilage-specific Gene, Chondromodulin-I, in Mesenchymal Stem Cells*[S]

Received for publication, February 24, 2010, and in revised form, July 21, 2010 Published, JBC Papers in Press, July 27, 2010, DOI 10.1074/jbc.M110.116319

Tomoki Aoyama[‡§¶], Takeshi Okamoto[‡§], Kenichi Fukiage[‡§], Seiji Otsuka[‡‖], Moritoshi Furu[‡§], Kinya Ito[‡‖], Yonghui Jin[‡], Michiko Ueda[‡], Satoshi Nagayama[**], Tomitaka Nakayama[§], Takashi Nakamura[§], and Junya Toguchida[‡§‡‡1]

From the [‡]Institute for Frontier Medical Sciences, the [‡‡]Center for iPS Cell Research and Application, Kyoto University, Kyoto 606-8507, the [§]Department of Orthopaedic Surgery, [¶]Human Health Sciences, and the [**]Department of Surgery and Surgical Basic Science, Graduate School of Medicine, Kyoto University, Kyoto 606-8507, Japan and the [‖]Department of Musculoskeletal Medicine, Graduate School of Medical Sciences, Nagoya City University, Nagoya 467-8601, Japan

Elucidating the regulatory mechanism for tissue-specific gene expression is key to understanding the differentiation process. The chondromodulin-I gene (*ChM-I*) is a cartilage-specific gene, the expression of which is regulated by the transcription factor, Sp3. The binding of Sp3 to the core-promoter region is regulated by the methylation status of the Sp3-binding motif as we reported previously. In this study, we have investigated the molecular mechanisms of the down-regulation of *ChM-I* expression in mesenchymal stem cells (MSCs) and normal mesenchymal tissues other than cartilage. The core-promoter region of cells in bone and peripheral nerve tissues was hypermethylated, whereas the methylation status in cells of other tissues including MSCs did not differ from that in cells of cartilage, suggesting the presence of inhibitory mechanisms other than DNA methylation. We found that a transcriptional repressor, YY1, negatively regulated the expression of *ChM-I* by recruiting histone deacetylase and thus inducing the deacetylation of associated histones. As for a positive regulator, we found that a transcriptional co-activator, p300, bound to the core-promoter region with Sp3, inducing the acetylation of histone. Inhibition of YY1 in combination with forced expression of p300 and Sp3 restored the expression of *ChM-I* in cells with a hypomethylated promoter region, but not in cells with hypermethylation. These results suggested that the expression of tissue-specific genes is regulated in two steps; reversible down-regulation by transcriptional repressor complex and tight down-regulation via DNA methylation.

The expression of cell lineage-specific genes is a key to initiating the differentiation of stem cells into a particular cell lineage, and the down-regulation of such genes in cells of other lineages is also critical to maintain a normal cellular physiology. The chondromodulin-I (*ChM-I*)[2] gene is a specific gene for cartilage tissue (1). We have found that the basal promoter activity of *ChM-I* is driven by a ubiquitous transcription factor, Sp3, and chondrocyte-specific expression is regulated by the methylation status of the Sp3-binding motif in the core-promoter region (2). Demethylation treatment *in vitro* restored the expression of *ChM-I* in cells of the osteogenic lineage (2, 3). A similar result was obtained with cells of the adipogenic lineage, in which the expression of an adipocyte-specific gene was restored in non-adipogenic cells by the elimination of methylated DNA in a regulatory region (4). Because DNA methylation is considered a tight epigenetic change under physiological conditions, it is a suitable mechanism for cells to inhibit the expression of unnecessary genes. It is, however, still to be investigated whether cells in tissues other than cartilage share the same inhibitory mechanism. It is also important to know how the expression of lineage-specific genes is down-regulated in tissue stem cells before differentiation is initiated. Mesenchymal stem cells (MSCs) in bone marrow are tissue stem cells, which can differentiate into multiple mesenchymal cell lineages including chondrogenic cells (5, 6). Because three-dimensional cultures supplemented with growth factors such as TGF-β can induce the chondrogenic differentiation of MSCs (6), there should be a mechanism other than DNA methylation to down-regulate the gene expression of *ChM-I* in undifferentiated MSCs. Modification of the histone tail is another mechanism regulating gene expression. The acetylation of histone H3 and H4 promotes gene expression, whereas deacetylation inhibits the expression (7). The dimethylation of histone H3 at lysine 9 (H3K9) in particular is correlated with DNA methylation and markedly inhibits gene expression (8, 9). These modifications of the histone tail and methylation status determine differentiation (10), and are regulated by several intrinsic histone modifiers including p300 and YY1 (11–13). p300 possesses intrinsic histone acetyltransferase (HAT) activity (11, 12). YY1 is a member of the polycomb group of transcription factors, which establish and maintain transcrip-

* This work was supported by Grants-in-aid for Scientific Research from the Japan Society for the Promotion of Science, from the Ministry of Education, Culture, Sports, Science, and Technology, and from the Ministry of Health, Labor, and Welfare.

[S] The on-line version of this article (available at http://www.jbc.org) contains supplemental Figs. S1 and S2.

[1] To whom correspondence should be addressed: Institute for Frontier Medical Sciences, Kyoto University, 53 Kawahara-cho, Shogoin, Sakyo-ku, Kyoto 606-8507, Japan. Tel.: 81-75-751-4134; Fax: 81-75-751-4646; E-mail: togjun@frontier.kyoto-u.ac.jp.

[2] The abbreviations used are: ChM, chondromodulin; MSC, mesenchymal stem cell; HAT, histone acetyltransferase; HDAC, histone deacetylase; OND, oligonucleotides.

tional silencing by recruiting histone deacetylase (HDAC) (13, 14). These intrinsic factors regulate the epigenetic status and regulate gene expression.

Here we demonstrated that the down-regulation of *ChM-I* expression by DNA methylation is restricted in particular cell types, whereas other cells including MSCs are free from the methylation, and found that expression of the *ChM-I* gene in these cells is reversibly dependent on histone modifications, which are regulated by the net activity of intrinsic histone modifiers, YY1 and p300.

EXPERIMENTAL PROCEDURES

Tissue Specimens and Primary Cultured Cells—Mesenchymal (cartilage, bone, fat, muscle, ligament, and tendon) and non-mesenchymal tissues (nerve, artery, and skin) were obtained from the lower limb of a 56-year-old male who underwent above-knee amputation. The tissues were frozen by dry ice and kept at −80 °C until nucleic acid extraction. Human primary cultured chondrocytes (hPCs) was isolated from same patient and cultured as previously mentioned (15). MSCs were isolated from the iliac bone of healthy donor as described (16). Normal human osteoblasts (NHOSTs) and human primary pre-adipocytes (hPAs) were obtained from TaKaRa (TaKaRa Bio, Shiga, Japan). All the primary cells were maintained in DMEM (Sigma-Aldrich) with 10% fetal bovine serum (Thermo Fisher Scientific Inc., Waltham, MA), 100 units/ml penicillin, and 100 mg/ml streptomycin, in 5% CO_2 at 37 °C. The Ethics Committee of the Faculty of Medicine, Kyoto University, approved the procedure and informed consent was obtained.

Cell Lines and Culture Conditions—The human cell lines, Saos2, were obtained from American Type Culture Collection (ATCC; Manassas, VA). The human osteosarcoma cell lines TAKAO and ANOS were established in our laboratory (2). All the cell lines used in this study were maintained in DMEM (Sigma-Aldrich) with 10% fetal bovine serum (Thermo Fisher Scientific Inc.), 100 units/ml penicillin, and 100 mg/ml streptomycin, in 5% CO_2 at 37 °C.

Antibodies and Expression Vectors—The following antibodies were used; anti-YY1 (sc-7341, Santa Cruz Biotechnology, Santa Cruz, CA), anti-p300 (05–257, Millipore Corp, Billerica, MA), anti-Sp3 (sc-644, Santa Cruz Biotechnology), anti-acetylated H3K9 (06–942, Millipore Corp), anti-dimethylated H3K9 (07–212, Millipore Corp), anti-pan H3 (07–690, Millipore Corp), and anti-HDAC2 (51–5100, Zymed Laboratory Inc., San Francisco, CA). Expression vectors for YY1 (pCEP-YY1) and p300 (pcDNA3-p300) were kindly provided by Drs. E. Seto and K. Miyazono, respectively. The Sp3 expression vector (pCMV-Sp3) was previously described elsewhere (17).

Reverse Transcription (RT)-PCR and Quantitative RT-PCR—RNA was isolated using the Rneasy kit (Qiagen KK, Tokyo, Japan) from frozen tissues and the cultured cell lines. All RT reactions were performed using 1 μg of total RNA with a Super Script First Strand Synthesis System for RT-PCR kit (Invitrogen, Carlsbad, CA). The relative amount of *ChM-I* mRNA was assessed by TaqMan real-time PCR with the ABI PRISM 7700 sequence detection system (Applied Biosystems, Foster City, CA) (2). A75-bp fragment from +411 (exon 4) to +485 (exon 5) of the *ChM-I* cDNA (GenBank™ accession number XM_007132) was amplified using specific primers (sense, 5′-GAAGGCTCGTATTCCTGAGGTG-3′; antisense, 5′-TGGCATGATCTTGCCTTCCAGT-3′) and labeled with a TaqMan probe (5′-FAM-CGTGACCAAACAGAGCATCTC-CTCCA-3′-TAMRA). 18 S rRNA was used as the internal control, and all reactions were run in duplicate. The ratio of *ChM-I*/18 S in each sample was calculated, and the expression level of *ChM-I* genes was demonstrated as a relative value using the *ChM-I*/18 S ratio in human articular cartilage as a standard (1.0) (2).

Drug Treatment—Cells (1×10^5) were seeded on 60-mm dishes in DMEM with 10% FBS. After they had attached to the dish, the cells were treated with either 5-*aza*-2′-deoxycytidine (5-*aza*-dC; Sigma-Aldrich) (1 μM) for 96 h or MS-275 (Nihon Scherring K.K., Chiba, Japan) (1 μM) for 24 h.

Bisulfite Genomic Sequencing—The bisulfite modification of DNA samples was performed using the EpiTect bisulfite kit (Qiagen). DNA (1 μg) was digested by BamHI for 12 h and subjected to sodium bisulfite treatment. Bisulfite-modified DNA-spanning residues −297 to −104 relative to the transcription start point (2) was amplified, cloned into the TA-vector (Invitrogen), and sequenced using an ABI 377 semiautomatic sequencer (Applied Biosystems).

Electrophoresis Mobility Shift Assay (EMSA)—Double-stranded DNA fragments corresponding to the sequence from −357 to −333 and from −86 to −44 were synthesized by annealing two single-stranded oligonucleotides (OND) (5′-CTTCACCTTCCATGAGCCATCTTC-3′ and 5′-GGGGGA-AGATGGCTCATGGAAGGT-3′; 5′-GGGCATCCGGGAG-TGCAGGACGAGCTTCCCGCGGCGGGA-3′; and 5′-TCT-CTCCCGCCGCGGGAAGCTCGTCCTGCACTCCCGGAT-3′, respectively) and filling in by DNA polymerase I (TOYOBO, Osaka, Japan). These fragments were designated GR3 and GR4 (Fig. 2*B*). For the formation of the complex, 5 μg of nuclear extract from cell lysate was incubated with ^{32}P end-labeled ONDs for 20 min at room temperature. The mixtures were electrophoresed in 5% polyacrylamide gel in 0.5× Tris borate EDTA at 45 volts for 3 h, and the gel then was dried and autoradiographed. For the competition assay, the OND-protein complex was produced in the same way in the presence of given amounts of non-labeled OND. In the supershift assay, nuclear extracts were incubated with 1 μg of anti-YY1 and anti-p300 antibody for 1 h on ice before being mixed with labeled DNA.

Luciferase Assay—The 533-bp fragment from −446 to +86 and 383-bp fragment from −296 to +86 relative to the transcription initiation site of the *ChM-I* gene was amplified by PCR, and cloned into a TA-vector using the TOPO cloning kit (Invitrogen). These fragments were subcloned into the luciferase reporter plasmid, PGV-B (Toyo Ink, Tokyo, Japan), yielding PGV-B-f1 and PGV-B-f1-del. Two tandem binding motifs of YY1 (*CCAT*) was mutated to (*TTAT*) by PCR, cloned into PGV-B, and designated PGV-B-f1-mt. One microgram of each reporter plasmid was co-transfected with 1 μg of pCEP-YY1 or pCMV-p300. Transfection efficiency was standardized by the co-transfection of 1 ng of pRL-TK control vector (Toyo Ink). Cells were harvested 24 h after transfection, and luciferase assays were performed with the

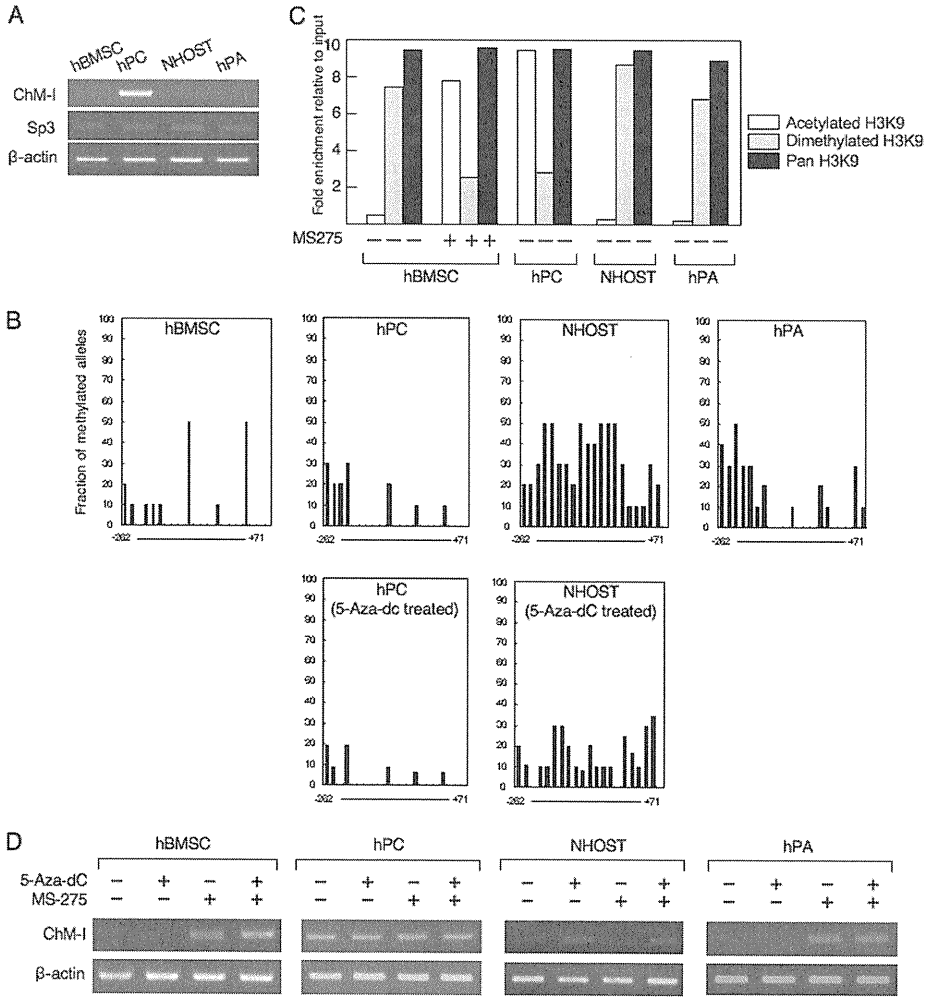

FIGURE 1. **DNA methylation and histone deacetylation down-regulate the expression of *ChM-I* in a cell type-specific manner.** *A*, expression of the *ChM-I* and *Sp3* genes in primary cultured mesenchymal cells. *B*, methylation status of the core-promoter region of *ChM-I*. The methylation of each CpG site was analyzed in 10 alleles by bisulfite genomic sequencing. The *y*-axis indicates the fraction of methylated alleles and the *x*-axis indicates the position of each CpG site relative to the transcription start site. Methylation status in hPC and NHOST treated with a demethylating reagent (5-*aza*-dC, 1 μM for 96 h) were also shown. *C*, ChIP-qPCR assay for the modification of histones in primary cultured mesenchymal cells. *Open box*, acetylated H3K9; *closed box*, dimethylated H3K9; *gray box*, Pan H3. Histone modification in hBMSC treated with an HDAC inhibitor (MS-275, 1 μM for 24 h) were also shown. The *y*-axis represents fold enrichment relative to input. *D*, expression of *ChM-I* after treatment with 5-*aza*-dC and/or MS-275.

PicaGene Dual SeaPansy system (Toyo Ink). Firefly-luciferase activity and SeaPansy-luciferase activity were measured as relative light units with a luminometer (STRATEC Biomedical Systems, Birkenfeld, Deutschland). The fold increase was calculated based on empty vector activity. Each experiment was performed in triplicate.

Chromatin Immunoprecipitation-Quantitative Polymerase Chain Reaction—The suitability of each antibody for the ChIP assay was confirmed by immunoprecipitation-Western blotting (data not shown). Tissue samples were treated using an EpiQuik tissue ChIP kit (Epigentek Group Inc. Brooklyn, NY). Cells were harvested and mixed with formaldehyde at a final concentration of 1.0% for 10 min at 37 °C to cross-link protein to DNA. Cells then were suspended in 0.2 ml of SDS lysis buffer and settled on ice for 10 min. DNA cross-linked with protein was sonicated into fragments of 200–1,000 bp. One-tenth of the sample was set aside as an input control, and the rest was precleared with salmon sperm DNA protein A-Sepharose beads (Millipore Corp) for 30 min with agitation. The soluble chromatin fraction was collected with each antibody at 4 °C overnight with rotation. Immune complexes were collected with salmon sperm DNA protein A-Sepharose beads and washed with the manufacturer's low salt, high salt, and LiCl buffers and then washed twice with TE buffer (10 mM Tris-HCl and 1 mM EDTA). The chromatin-antibody complexes were eluted with elution buffer (1% SDS and 0.1 M $NaHCO_3$). Protein DNA cross-links were reversed with 5 M NaCl at 65 °C for 4 h, proteinase K treatment and phenol-chloroform extraction were carried out, and then the DNA was precipitated in ethanol. The DNA pool from ChIP, input control and negative control was used for quantitative PCR. PCR amplification was performed on an ABI 7700 real-time PCR (Applied Biosystems). PCR amplification was performed using primers specific for the *ChM-I* regulatory region (sense, 5′-GAATGCAGGCCAGTGAGAAGGT-3′;1 antisense, 5′-GCACCCTGGGATCTGTCCCGCT-3′, Fig. 2*B*). The PCR conditions were an initial step of 5 min at 95 °C, followed by 40 cycles of 15 s at 95 °C, 10 s at 64 °C and 60 s at 72 °C. Primers were designed according to the selected genes for evaluating ChIP. To generate a standard curve for each amplicon, threshold cycle (CT) values of serially diluted input DNA, which were extracted in the ChIP experiment, were determined. The status of histone modification and binding of HDAC2, p300, YY1, and Sp3 changes were determined using the 2(-Delta Delta C(T)) method (18). They were demonstrated as a relative value using the enrichment of IP DNA/input DNA. A melting curve analysis was performed for each reaction to ensure a single peak. Each experiment was performed in triplicate, with the values averaged to obtain 1 datum per sample.

siRNAs—Luciferase siRNA duplex (GL2RN1, Dharmacon) was used as a negative control. 40 μM siRNA for YY1 (GeneSolution siRNA; Hs-YY1–5, Qiagen), p300 (p300 Pub. siRNA, Duplex1, Qiagen), and Sp3 (previously described in (2)) were transfected by Lipofection LTX (Invitrogen). RNA was prepared 48 h after transfection and used for the RT-PCR.

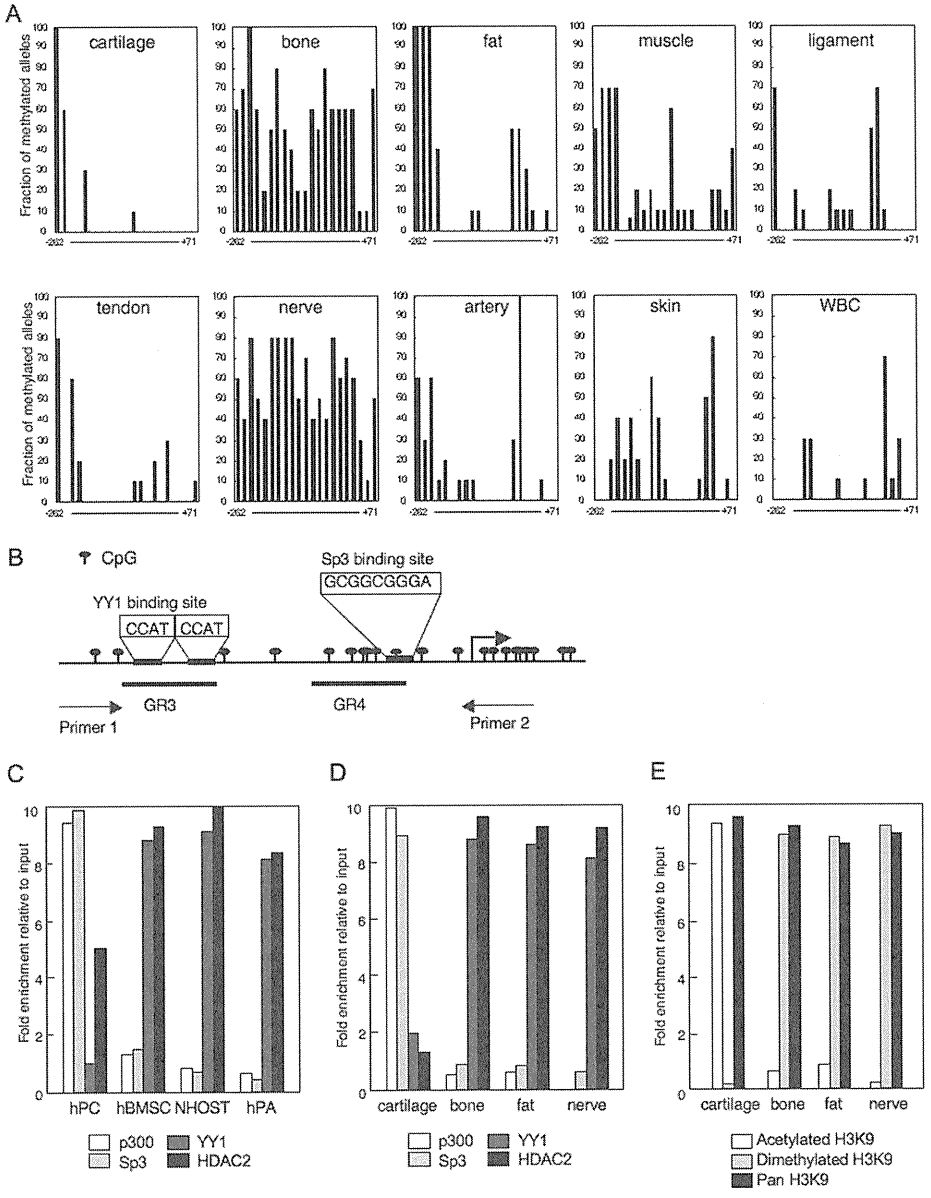

FIGURE 2. **Binding of YY1 and p300 determined the modification of H3K9 and the mRNA expression of *ChM-I* in mesenchymal tissues.** *A*, methylation status of the core-promoter region of the *ChM-I*. DNA extracted from normal tissue was analyzed by bisufite genomic sequencing. *B*, genomic structure of the core-promoter region of *ChM-I*. CpG sites from −262 to +71 were marked as indicated, and the transcription start site is indicated by an *arrow*. Two overlapping YY1-binding motifs (−344 to −347 and −342 to −346), and an Sp3-binding motifs (−56 to −48) are also indicated. A DNA fragment for the ChIP assay was amplified by primer 1 (−446 to −425) and primer 2 (+70 to +91). GR3 (−357 to −337) and GR4 (−86 to −44) were OND probes used in the EMSA for YY1 and p300, respectively. ChIP-qPCR assay for the binding of transcriptional regulators in primary cultured cells (*C*) and cells of normal tissues (*D*). The *y*-axis represents fold enrichment relative to input. *E*, ChIP-qPCR assay for the modification of histones in normal tissues.

RESULTS

DNA Methylation and Histone Deacetylation Down-regulate the Expression of ChM-I in a Cell Type-specific Manner—The expression of *ChM-I* was analyzed by RT-PCR in primary-cultured mesenchymal cells (hMSCs, hPCs, NHOSTs, and hPAs), among which only hPCs expressed the gene (Fig. 1*A*). We have previously shown the expression of *ChM-I* to be induced by the binding of Sp3, which was regulated by the methylation status of the binding motif in the core-promoter region (2). Expression levels of the *Sp3* gene did not differ among the four types of cells (Fig. 1*A*). The core-promoter region of *ChM-I* was hypomethylated in hPCs and hypermethylated in NHOSTs (Fig. 1*B*), which was consistent with the positive and negative expression of *ChM-I* in each cell. The methylation status of the core-promoter region of hMSCs or hPAs, however, was not significantly different from that of hPCs in spite that the expression of *ChM-I* was not detected in these cells (Fig. 1*B*). We have also shown that the acetylation of histone H3 at lysine 9 (H3K9) is necessary to induce the binding of Sp3 to the core-promoter region of *ChM-I*. ChIP analyses showed that H3K9 associated with the core-promoter region was acetylated in hPCs, but dimethylated in hMSCs, NHOSTs, and hPAs (Fig. 1*C*). Treatment with a demethylation reagent (5-*aza*-dC) induced the expression of *ChM-I* in NHOSTs (Fig. 1*D*), which was associated with demethylatiion in the promoter region of the *ChM-I* gene (Fig. 1*B*, *lower panel*). 5-*aza*-dC treatment, however, showed no effects in hMSCs or hPAs (Fig. 1*D*). On the other hand, treatment with a HDAC inhibitor (MS-275) induced the expression of *ChM-I* gene in hMSCs and hPAs, but not in NHOSTs (Fig. 1*D*). The induction of ChM-1 gene expression in hMSC was associated with the acetylation of H3K9 (Fig. 1*C*). These results suggested two mechanisms for the down-regulation of *ChM-I* expression in primary-cultured cells; methylation of the core-promoter region as found in NHOSTs, and histone deacetylation and methylation without DNA methylation as found in hMSCs and hPAs.

The Binding of YY1 and p300 Correlates to the Expression of ChM-I in Normal Mesenchymal Tissues—Among the normal mesenchymal tissues examined, the expression of *ChM-I* was observed only in cartilage (supplemental Fig. S1). The methylation status of the core-promoter region, however, differed significantly among tissues (Fig. 2*A*). DNA extracted from cells in cartilage and fat tissues showed a hypomethylated state in the core-promoter region, which was similar to those found in hPCs and hPAs (Fig. 1*B*). DNA extracted from cells in bone and nerve tissues showed

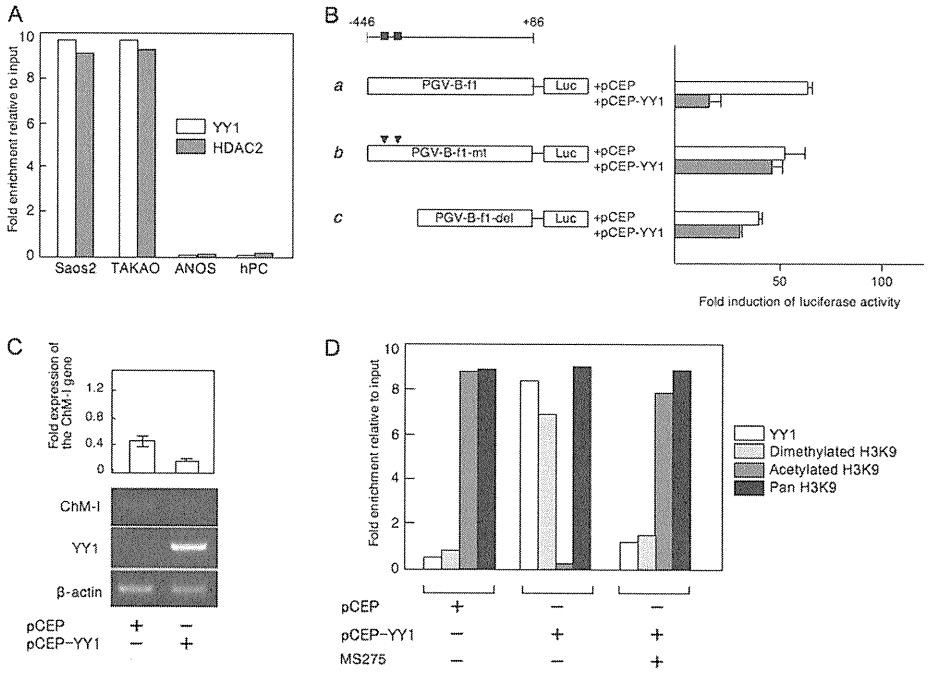

FIGURE 3. **YY1 bound to the regulatory region of *ChM-I* and decreased the promoter activity of *ChM-I*.** *A*, ChIP-qPCR assay for YY1 and HDAC2. *B*, luciferase reporter assay. *a*, DNA fragment encompassing −446 to +86 was cloned into a reporter vector containing the luciferase gene (*PGV-B-f1*). The *black box* indicates the location of the consensus sequence for the YY1-binding motif. *b*, PGV-B-f1-mt contains mutations in the YY1-binding motif (*arrowhead*), and PGV-B-f1-del lacked the YY1-binding motifs (*c*). Each reporter vector was co-transfected with empty vector (*pCEP*) or the YY1 expression vector (*pCEP-YY1*) into ANOS. The fold-increase was calculated based on empty vector activity. *C*, expression of endogenous *ChM-I* in hPCs transfected with the YY1 expression vector. The expression of *ChM-I* was semi-quantified taking the value for endogenous expression as 1.0 and is demonstrated at the *top*. *D*, ChIP-qPCR assay of hPCs transfected with the YY1 expression vector with or without MS275 treatment (1 μM for 24 h). Forced expression of YY1 in hPCs changed the modification of the H3 tail from acetylation to dimethylation.

that the core-promoter region was hypermethylated, which was similar to those that found in NHOSTs (Fig. 1*B*). In other tissues, the core-promoter region was hypomethylated. These results further suggested a mechanism other than DNA methylation to down-regulate the expression of *ChM-I*.

A search for factors regulating the chromatin structure revealed two tandem repeats (−344 to −347 and −342 to −346) of the binding motif of YY-1, which represses gene expression by recruiting HDAC to target regions (13, 14). As for factors with HAT activity, we focused on p300, which is known to relieve the transcriptional repression by YY1 (19). p300 also plays a role as a transcriptional adaptor recruiting transcription factors such as Sp3 (20). ChIP-qPCR assay showed that YY1 and HDAC2 bound to the core-promoter region in ChM-I-negative hMSCs, NHOSTs, and hPAs, whereas p300 and Sp3 bound in ChM-I-positive hPC (Fig. 2*C*). Consistent with the results obtained with primary-cultured cells, p300 and Sp3 bound to the core-promoter region in cells of cartilage, but not bone, fat or nerve tissue (Fig. 2*D*). On the other hand, the binding of YY1 and HDAC2 was observed in cells of bone, fat, and nerve, but not cartilage (Fig. 2*D*). ChIP-qPCR assay of the histone tail associated with the core-promoter region demonstrated that H3K9 was acetylated in cells of cartilage tissue, and dimethylated in those of bone, fat, and nerve tissues (Fig. 2*E*), which corresponded with the expression of *ChM-I* in each tissue. These results indicated that the expression of *ChM-I* correlated positively with the binding of p300 and negatively with that of YY1.

YY1 Binds to the Core Promoter Region and Inhibits Transcription—To further analyze the involvement of YY1 and p300 in the regulation of *ChM-I*, we used an osteosarcoma cell line, ANOS, as a ChM-I positive cell line, which we have previously investigated. The core-promoter region of the gene was hypomethylated in ANOS cells (2). As ChM-I-negative cell lines, two other osteosarcoma cell lines, Saos2 and TAKAO, were used, in which the core-promoter region was hypermethylated (2).

ChIP-qPCR assays showed that YY1and HDAC2 bound to the regulatory region of Saos2 and TAKAO cells, but not ANOS cells and hPCs (Fig. 3*A*). The binding of YY1 was further confirmed by an EMSA using an oligonucleotide (OND) (GR3) containing putative YY1-binding motifs (−342 to −347) (supplemental Fig. S2*A*). A shifted band was detected in the protein-OND complex from Saos2 cells, which disappeared on competition with unlabeled OND (supplemental Fig. S2*A*, *left panel*). The shifted band was detected also in the protein-OND complex from TAKAO cells, but not in ChM-I-positive cells (ANOS cells and hPCs) (supplemental Fig. S2*A*, *middle panel*). The shifted band was further shifted by the pretreatment with anti-YY1 antibody (supplemental Fig. S2*A*, *right panel*). These results indicated that YY1 bound to the core-promoter region of *ChM-I* in ChM-I-negative cells. To analyze the functional involvement of YY1, a reporter assay using the promoter fragment (−446 to +86) was performed (Fig. 3*B*), which contained the basal transcriptional activity of *ChM-I* (2). When the YY1 expression vector was co-transfected with the reporter plasmid, the promoter activity was significantly inhibited in ANOS cells (Fig. 3*B*, *a*). This inhibitory effect of YY1 was not observed when the reporter vector was replaced with one containing mutations in the YY1 motif (Fig. 3*B*, *b*) or lacking the motif (Fig. 3*B*, *c*). Forced expression of YY1 inhibited the expression of the endogenous *ChM-I* gene in hPCs (Fig. 3*C*), which was associated with the deacetylation and dimethylation of H3 (Fig. 3*D*). Co-treatment with MS275 inhibited the effect of forced expression of YY-1, rescuing the acetylation of H3K9 (Fig. 3*D*). These results suggested that YY1 inhibits the transcriptional activity of *ChM-I* by binding to a putative binding motif in the core-promoter region.

p300 Binds to the Core Promoter Region and Enhances Transcription—ChIP-qPCR assays showed that p300 as well as Sp3 bound to the core-promoter region of *ChM-I* in ANOS cells and hPCs, but not Saos2 and TAKAO cells (Fig. 4*A*). H3K9 associated with this region was acetylated in ANOS cells and

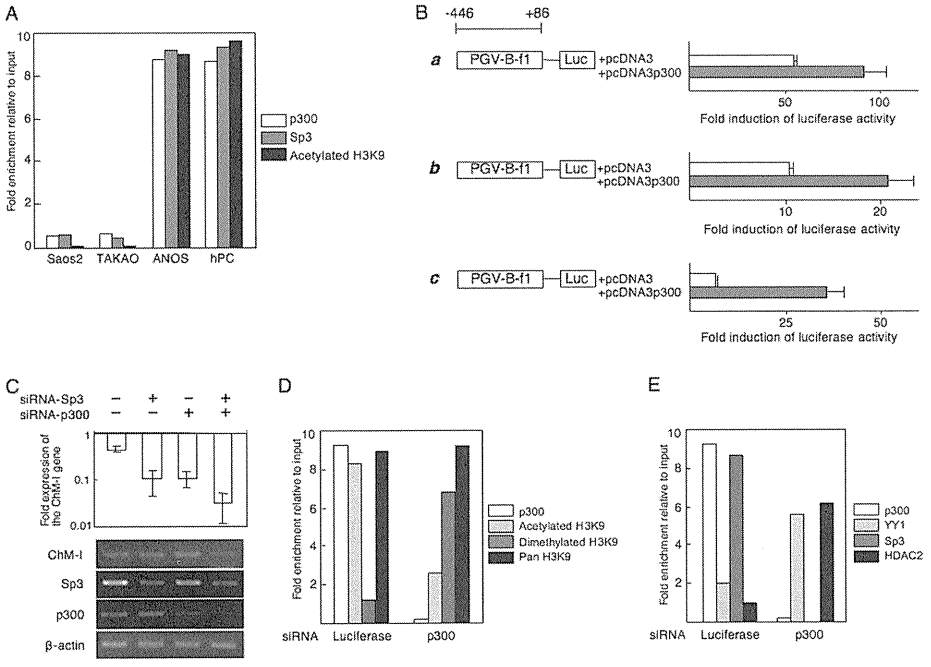

FIGURE 4. **p300 binds to the core promoter region and enhances transcription.** *A*, ChIP-qPCR assay of p300, Sp3 and acetylated H3. *B*, luciferase reporter assay. The reporter construct was described in the legend for Fig. 3*B*, and co-transfected with empty vector (pcDNA3) or the p300 expression vector (pcDNA3-p300) into ANOS (*a*), Saos2 (*b*), or TAKAO (*c*). The fold-increase was calculated based on empty vector activity. *C*, down-regulation of ChM-I gene expression by siRNA for Sp3 and/or p300. siRNAs for Sp3 and/or p300 were transfected into ANOS, and the expression of ChM-I, Sp3, and p300 was analyzed by RT-PCR. The expression of *ChM-I* was semi-quantified taking the value for endogenous expression as 1.0 and is demonstrated at the *top*. *D*, ChIP-qPCR assay for the modification of H3K9 (*D*) and for the binding of transcription regulators (*E*): cross-linked DNA-protein complexes were prepared from ANOS treated with or without siRNA for p300 and used for ChIP-qPCR assay.

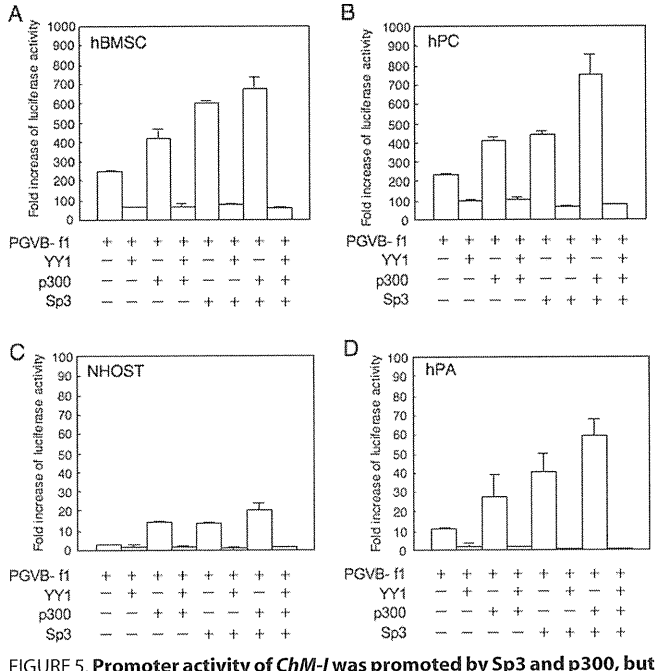

FIGURE 5. **Promoter activity of *ChM-I* was promoted by Sp3 and p300, but completely inhibited by YY1 in primary cultured cells.** The luciferase reporter vector containing the core-promoter fragment of the *ChM-I* gene (*PGV-B-f1*) was co-transfected with YY1, p300 and/or Sp3 expression vectors into hMSCs (*A*), hPCs (*B*), NHOSTs (*C*), and hPAs (*D*). The fold-increase was calculated based on empty vector activity.

hPCs, but not Saos2 or TAKAO cells (Fig. 4*A*). The binding of p300 was further confirmed by an EMSA using an OND (GR4)-containing putative p300 and Sp3-binding motifs (−56 to −48) (supplemental Fig. S2*B*). A shifted band was observed in extracts from ANOS cells, but not Saos2 or TAKAO cells (supplemental Fig. S2*B*, *middle panel*). The specificity of the band was confirmed by addition of a cold OND (supplemental Fig. S2*B*, *left panel*). The shifted band was supershifted when cell extracts were pretreated with anti-Sp3 antibody, and the same band disappeared when cell extracts were pretreated with anti-p300 antibody (supplemental Fig. S2*B*, *right panel*), suggesting that the protein-OND complex contained both Sp3 and p300. The functional involvement of p300 was analyzed with a promoter assay. Promoter activity was increased by co-transfection of the p300 expression vector in both ChM-I-positive (ANOS, Fig. 4*B*, *a*) and negative (Saos2, Fig. 4*B*, *b*; TAKAO, Fig. 4*B*, *c*) cells. Inhibition of p300 or Sp3 expression by the siRNA for each gene (siRNA-p300 and siRNA-Sp3) reduced the expression of *ChM-I* in hPCs, while the two siRNAs combined had an additive effect (Fig. 4*C*). ChIP-qPCR assays showed that the siRNA for p300 changed H3K9 from an acetylated to dimethylated form (Fig. 4*D*). These results suggest that p300 positively regulates the transcriptional activity of *ChM-I* by inducing the acetylation of H3K9 associated with this region.

Involvement of YY1 and p300 in Primary Mesenchymal Cells—The effect of YY1 and p300 on promoter activity was further analyzed in primary-cultured mesenchymal cells (Fig. 5). Surprisingly, the transcriptional activity of the basal promoter fragment in hMSCs (Fig. 5*B*) was as strong as those in hPCs (Fig. 5*A*), although the expression of endogenous *ChM-I* was weak in hMSCs. In contrast, the basal activity level was low in NHOSTs and hPAs (Fig. 5, *C* and *D*). When the YY1 expression vector was co-transfected with the reporter vector, promoter activity was significantly inhibited in all strains (Fig. 5, *A–D*). Co-transfection with the p300 or Sp3 expression vector enhanced the activity, and simultaneous transfection of the two vectors increased it in an additive manner (Fig. 5, *A–D*). The enhancement of *ChM-I* expression by the p300 and/or Sp3 expression vectors was completely inhibited by the co-transfection of YY1 in all strains (Fig. 5, *A–D*). These results confirmed that YY1 and p300 are involved in the regulation of *ChM-I* transcription in mesenchymal cells, and that because this luciferase reporter system has no relationship with histone modifications, YY1

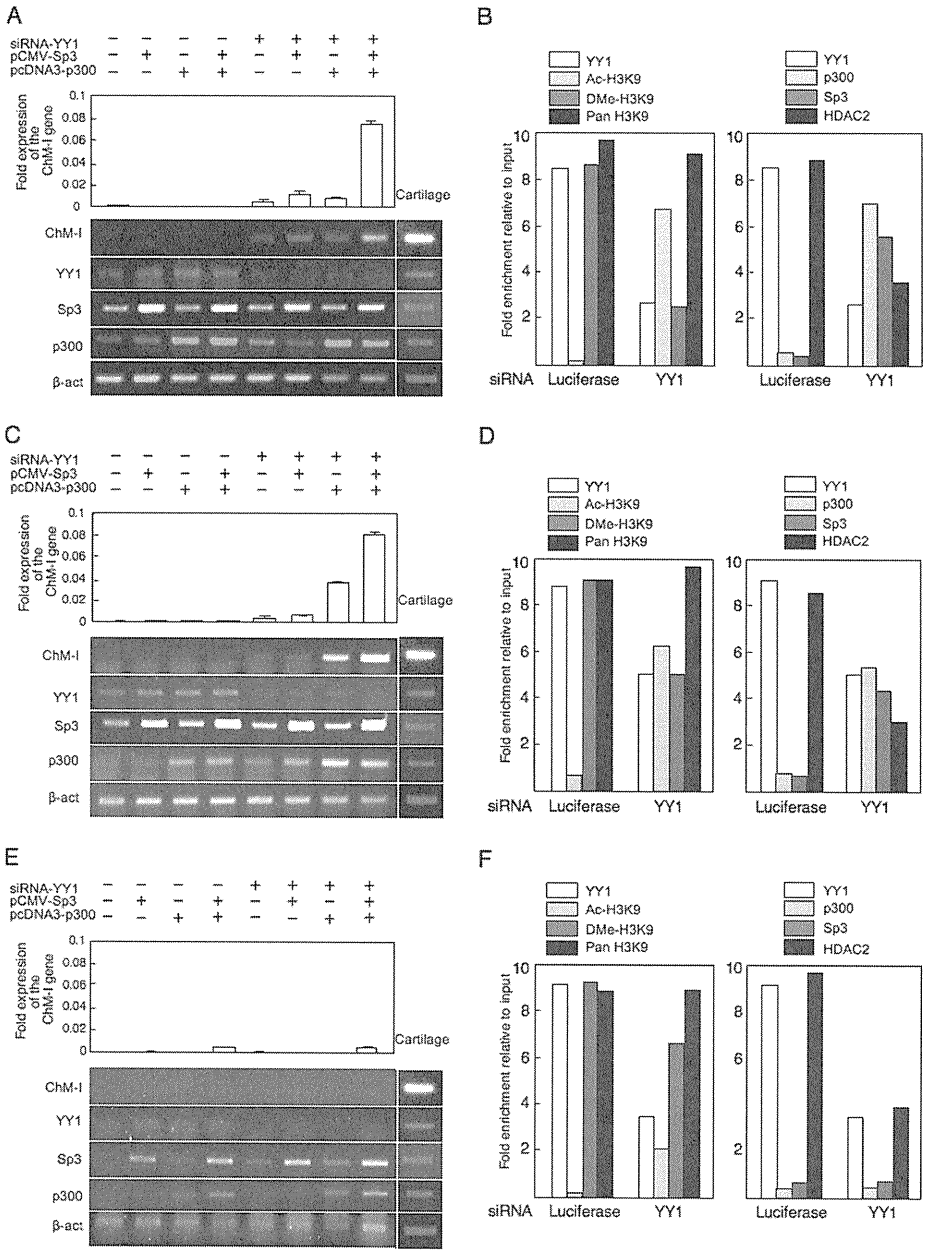

FIGURE 6. **Induction of *ChM-I* expression in ChM-I-negative primary cultured cells by modification of regulators.** *A–C*, primary-cultured cells were transfected with a combination of the siRNA for YY1, p300 expression vector, and Sp3 expression vector, and mRNA level of *ChM-1*, *YY1*, *p300*, and *Sp3* gene were analyzed by semi-quantitative RT-PCR (*lower panel*). The expression of the *ChM-I* was further analyzed by quantitative RT-PCR and digitalized (*upper panel*). *A*, hMSCs; *C*, hPAs; *E*, NHOSTs. ChIP-qPCR assay: *B*, hMSCs; *D*, hPAs; *F*, NHOSTs. Cross-linked DNA-protein complexes were prepared from primary cultured cells treated with or without siRNA for YY1 and used for ChIP-qPCR assay for the modificationf H3K9 (*left panels*) and for the binding of transcription regulators (*right panels*).

may directly inhibit the function of p300 or p300/Sp3 complex in addition to the modification of chromatin structure.

Cell-specific Effects of YY1 Inhibition on the Expression of ChM-I—Finally, the effect of YY1 expression on endogenous ChM-I expression was evaluated using siRNA for the gene (siRNA-YY1). In hMSCs (Fig. 6*A*), the inhibition of YY1 expression slightly induced the expression of *ChM-I* gene. The introduction of the p300 and/or Sp3 expression vectors had little effect on the expression of *ChM-I*, but significantly up-regulated it when combined with siRNA-YY1. Similar results were obtained in hPAs (Fig. 6*C*). In both cell types, siRNA-YY1 treatment induced the acetylation of H3K9 along with reductions in the dimetylation of H3K9 (Fig. 6, *B* and *D*, *left panels*). At the same time, siRNA-YY1 treatment dissociated HDAC2 and recruited p300 and Sp3 in the core-promoter region of *ChM-I* (Fig. 6, *B* and *D*, *right panels*). In NHOSTs (Fig. 6*E*), however, the combination the inhibition of YY1 and over-expression of p300 and Sp3 showed little effect for the induction of *ChM-I* expression. siRNA-YY1 treatment failed to induce the acetylation of H3K9 (Fig. 6*F*, *left panel*). Interestingly, although p300 was successfully recruited to the promoter region, no binding of Sp3 was observed in NHOSTs (Fig. 6*F*, *right panel*). These results suggested that Sp3 and p300 independently bind to the promoter region, and the binding of Sp3 was inhibited by the methylation of target DNA, but that of p300 was not. Therefore, the expression of a cartilage-specific gene, *ChM-I*, can be induced in some types of mesenchymal cells including MSCs by the modification of repressors (YY1) and activators (p300), but not in other cells, in which the expression is irreversibly inhibited by DNA methylation.

DISCUSSION

Numerous studies support the importance of epigenetic status for the regulation of differentiation, based on experiments involving chemical modifications of genome and the winding protein histone (21, 22). DNA methylation at CpG dinucleotides is a major epigenetic modification of the genome and associated with gene silencing (23). Because no intrinsic DNA-demethylating enzyme has been found, the inhibition by DNA methylation is tight under physiological conditions. Genomic DNA of embryonic stem (ES) cells is hypomethylated, and the total amount of methylated DNA increases with development (22, 24). Thus DNA methylation is a key mechanism to regulate and maintain the expression of cell type-specific genes. Unexpectedly, however, the methylation in the core-promoter region played a role in inhibiting the expression of *ChM-I* only

in particular types of mesenchymal cells; cells in bone (mainly osteocytes and osteoblasts) and peripheral nerve (mainly Schwann cells and perineural cells) (Fig. 2*A*). The hypomethylated status in hMSCs is reasonable considering the potential of these cells to differentiate. However, the core-promoter in terminally differentiated cells of a remote cell-lineage such as white blood cells was free from methylation and thus in a reversible state for gene expression (Fig. 2*A*). At present, we have no data to explain why some types of cells use DNA methylation to inhibit the expression of *ChM-I* and others do not. Cells of chondrogenic and osteogenic lineages are closely related, and may share a considerable proportion of transcriptional machinery. Therefore DNA methylation might be required to inhibit the expression of genes specific to chondro- or osteogenic lineages. The reporter assay gave almost identical results in hMSCs as in hPCs (Fig. 5, *A* and *B*), indicating that transcriptional machinery n hMSC to be ready to induce the expression of *ChM-I*, although there is no endogenous expression of the gene. This result strongly suggested that epigenetic machinery regulated the lineage-specific gene expression in stem cells.

The epigenetic status of each cell had been considered static, but recent a study demonstrated a dynamic nature to these modifications (25). We and others gave examples in which modification of the histone code induced a change of DNA methylation (3, 26). Notably, the modification of H3K9 strongly correlated with DNA methylation; dimethylated H3K9 correlated with hypomethylation and deacetylated H3K9 correlated with hypermethylation (9, 27). The recent discovery that the forced expression of transcription factors can reverse the epigenetic status of differentiated to that of ES cells is an extreme example of the dynamic nature of epigenetic status (28, 29). We showed that the expression of *ChM-I* was down-regulated by histone modifications in stem cells and some types of differentiated cells. The epigenetic status is induced and maintained by a number of intrinsic histone modifiers (30). In this study, we found that YY1 and p300 are main modifiers of histone associated with the core-promoter region of the ChM-I gene. YY1 is a DNA-binding zinc finger transcription factor, which has dual functions as an activator and a repressor (14). YY1 inhibits the transcription of target genes by competing for DNA-binding sites with activators, binding directly to activators, or recruiting co-repressors (14). One of these co-repressors is HDAC2, which was first identified as a binding partner of YY1 (13, 14). Previously, we demonstrated that HDAC2 bound to a histone tail associated with the core-promoter region of *ChM-I* in ChM-I-negative cells (3). In the present study, we showed that forced expression of YY1 deacetylated H3 associated with the core-promoter region in *ChM-I* (Fig. 3*E*), whereas HDAC2 was dissociated by the inhibition of YY1, causing acetylation of H3 (Fig. 6, *B*, *D*, and *F*). These results indicated that YY1 repressed the expression of *ChM-I* by recruiting HDAC2 to induce deacetylation of H3. Another repressive mechanism is the direct binding of p300, a binding partner of YY1 (14). p300 acts as an activator for target gene expression through intrinsic HAT activity (11, 12). Inhibition of p300 by siRNA resulted in the deacetylation of H3 and the repression of *ChM-I* expression (Fig. 5*C*), indicating the role of p300 as HAT for *ChM-I* expression. p300 also acts as a transcriptional co-activator for Sp3, not Sp1 (19), which is the main transcription factor of *ChM-I* (2). The exogenous expression of p300 enhanced the promoter activity in the reporter assay, suggesting the role of p300 as a co-activator. Inhibition of the promoter activity by the YY1 expression vector in the reporter assay indicated that YY1 acted as a direct repressor for p300 in addition to acting as a recruiter of HDAC (Fig. 6, *A*, *C*, and *E*). These results suggested that YY1 and p300 are involved in the regulation of *ChM-I* expression through the modification of histones and also the regulation of each others function.

It remains unclear how the repression of YY1 is relieved in chondrogenic cells. One possible mechanism is a post-translational modification of the YY1 protein. YY1 is glycosylated by *O*-linked *N*-acetylglucosaminylation, and glycosylated YY1 fails to bind to DNA (31). *O*-linked glucosamine is expressed in cartilage tissue (32). Such tissue-specific modifications may determine the expression of tissue-specific genes. It is also likely that tissue-specific chromatin-remodeling factors other than YY1 and p300 are involved in the regulation. Analyzing these issues may help to elucidate how the direction of differentiation is determined in stem cells.

Acknowledgments—We thank Dr. M. Nakanishi for providing MS-275 and helpful suggestions, Dr. K. Miyazono for the p300 expression vector, and Dr. E. Seto for the YY1 expression vector.

REFERENCES

1. Hiraki, Y., Tanaka, H., Inoue, H., Kondo, J., Kamizono, A., and Suzuki, F. (1991) *Biochem. Biophys. Res. Commun.* **175,** 971–977
2. Aoyama, T., Okamoto, T., Nagayama, S., Nishijo, K., Ishibe, T., Yasura, K., Nakayama, T., Nakamura, T., and Toguchida, J. (2004) *J. Biol. Chem.* **279,** 28789–28797
3. Aoyama, T., Okamoto, T., Kohno, Y., Fukiage, K., Otsuka, S., Furu, M., Ito, K., Jin, Y., Nagayama, S., Nakayama, T., Nakamura, T., and Toguchida, J. (2008) *Biochem. Biophys. Res. Commun.* **365,** 124–130
4. Noer, A., Sorensen, A. L., Boquest, A. C., and Collas, P. (2006) *Mol. Biol. Cell.* **17,** 3543–3556
5. Caplan, A. I. (1991) *J. Orthop. Res.* **9,** 641–650
6. Pittenger, M. F., Mackay, A. M., Beck, S. C., Jaiswal, R. K., Douglas, R., Mosca, J. D., Moorman, M. A., Simonetti, D. W., Craig, S., and Marshak, D. R. (1999) *Science* **284,** 143–147
7. Grunstein, M. (1997) *Nature* **389,** 349–352
8. Zhao, W., Soejima, H., Higashimoto, K., Nakagawachi, T., Urano, T., Kudo, S., Matsukura, S., Matsuo, S., Joh, K., and Mukai, T. (2005) *J. Biochem.* **137,** 431–440
9. Kondo, Y., Shen, L., and Issa, J. P. (2003) *Mol. Cell. Biol.* **23,** 206–215
10. Gan, Q., Yoshida, T., McDonald, O. G., and Owens, G. K. (2007) *Stem Cells* **25,** 2–9
11. Ogryzko, V. V., Schiltz, R. L., Russanova, V., Howard, B. H., and Nakatani, Y. (1996) *Cell* **87,** 953–959
12. Bannister, A. J., and Kouzarides, T. (1996) *Nature* **384,** 641–643
13. Yang, W. M., Yao, Y. L., Sun, J. M., Davie, J. R., and Seto, E. (1997) *J. Biol. Chem.* **272,** 28001–28007
14. Gordon, S., Akopyan, G., Garban, H., and Bonavida, B. (2006) *Oncogene* **25,** 1125–1142
15. Aoyama, T., Liang, B., Okamoto, T., Matsusaki, T., Nishijo, K., Ishibe, T., Yasura, K., Nagayama, S., Nakayama, T., Nakamura, T., and Toguchida, J. (2005) *J. Bone. Miner. Res.* **20,** 377–389
16. Shibata, K. R., Aoyama, T., Shima, Y., Fukiage, K., Otsuka, S., Furu, M., Kohno, Y., Ito, K., Fujibayashi, S., Neo, M., Nakayama, T., Nakamura, T., and Toguchida, J. (2007) *Stem Cells.* **25,** 2371–2382

17. Suske, G. (1999) *Gene* **238,** 291–300
18. Livak, K. J., and Schmittgen, T. D. (2001) *Methods* **25,** 402–408
19. Lee, J. S., Galvin, K. M., See, R. H., Eckner, R., Livingston, D., Moran, E., and Shi, Y. (1995) *Genes Dev.* **9,** 1188–1198
20. Kishikawa, S., Murata, T., Kimura, H., Shiota, K., and Yokoyama, K. K. (2002) *Eur. J. Biochem.* **269,** 2961–2970
21. Spivakov, M., and Fisher, A. G. (2007) *Nat. Rev. Genet.* **8,** 263–271
22. Bernstein, B. E., Meissner, A., and Lander, E. S. (2007) *Cell* **128,** 669–681
23. Esteller, M. (2007) *Nat. Rev. Genet.* **8,** 286–298
24. Reik, W., Dean, W., and Walter, J. (2001) *Science* **293,** 1089–1093
25. Klose, R. J., and Zhang, Y. (2007) *Nat. Rev. Mol. Cell Biol.* **8,** 307–318
26. Nakao, M. (2001) *Gene* **278,** 25–31
27. Rougeulle, C., Chaumeil, J., Sarma, K., Allis, C. D., Reinberg, D., Avner, P., and Heard, E. (2004) *Mol. Cell. Biol.* **24,** 5475–5484
28. Takahashi, K., Tanabe, K., Ohnuki, M., Narita, M., Ichisaka, T., Tomoda, K., and Yamanaka, S. (2007) *Cell* **131,** 861–872
29. Okita, K., Ichisaka, T., and Yamanaka, S. (2007) *Nature* **448,** 313–317
30. Pasini, D., Bracken, A. P., Agger, K., Christensen, J., Hansen, K., Cloos, P. A., and Helin, K. (2008) *Cold Spring Harb. Symp. Quant. Biol.***73,** 253–263
31. Hiromura, M., Choi, C. H., Sabourin, N. A., Jones, H., Bachvarov, D., and Usheva, A. (2003) *J. Biol. Chem.* **278,** 14046–14052
32. Thonar, E. J., Lohmander, L. S., Kimura, J. H., Fellini, S. A., Yanagishita, M., and Hascall, V. C. (1983) *J. Biol. Chem.* **258,** 11564–11570

arthritis research&therapy

RESEARCH ARTICLE Open Access

Prostaglandin E2 receptor type 2-selective agonist prevents the degeneration of articular cartilage in rabbit knees with traumatic instability

Hiroto Mitsui[1,3], Tomoki Aoyama[1,4*], Moritoshi Furu[1,2], Kinya Ito[1,3], Yonghui Jin[1], Takayuki Maruyama[5], Toshiya Kanaji[5], Shinsei Fujimura[5], Hikaru Sugihara[5], Akio Nishiura[5], Takanobu Otsuka[3], Takashi Nakamura[2] and Junya Toguchida[1,2,6]

Abstract

Introduction: Osteoarthritis (OA) is a common cause of disability in older adults. We have previously reported that an agonist for subtypes EP2 of the prostaglandin E2 receptor (an EP2 agonist) promotes the regeneration of chondral and osteochondral defects. The purpose of the current study is to analyze the effect of this agonist on articular cartilage in a model of traumatic degeneration.

Methods: The model of traumatic degeneration was established through transection of the anterior cruciate ligament and partial resection of the medial meniscus of the rabbits. Rabbits were divided into 5 groups; G-S (sham operation), G-C (no further treatment), G-0, G-80, and G-400 (single intra-articular administration of gelatin hydrogel containing 0, 80, and 400 μg of the specific EP2 agonist, ONO-8815Ly, respectively). Degeneration of the articular cartilage was evaluated at 2 or 12 weeks after the operation.

Results: ONO-8815Ly prevented cartilage degeneration at 2 weeks, which was associated with the inhibition of matrix metalloproteinase-13 (MMP-13) expression. The effect of ONO-8815Ly failed to last, and no effects were observed at 12 weeks after the operation.

Conclusions: Stimulation of prostaglandin E2 (PGE2) via EP2 prevents degeneration of the articular cartilage during the early stages. With a system to deliver it long term, the EP2 agonist could be a new therapeutic tool for OA.

Keywords: prostaglandin E2, EP_2, ONO-8815Ly, osteoarthritis, ACLMT

Introduction

Osteoarthritis (OA) is the single most common cause of disability in older adults [1]. It is a complex process involving a combination of cartilage degradation, repair, and inflammation. However, its pathogenesis is not yet fully understood [2]. Articular cartilage is composed of chondrocytes, and an extensive extracellular matrix (ECM). The major ECM components are type II collagen and aggrecan. In normal cartilage, catabolic and anabolic activities are in dynamic equilibrium. Chondrocytes can produce several catabolic cytokines such as IL-1 and TNF-α, which in turn induce the production of proteinases including matrix metalloproteinases (MMPs) and disintegrin-like and metalloproteinase with thrombospondin, that lead to the destruction of the matrix network [3,4]. Among the MMPs, MMP-13 (collagenase 3) plays a particularly important role in causing OA [5]. Indeed, transgenic mice carrying an inducible human *MMP-13* gene develop pathological changes similar to those observed in human OA patients, when the transgene is expressed in articular cartilages of postnatal mice [6]. Moreover, inhibitors of MMP-13 prevent the degradation of articular cartilage [5,7]. Chondrocytes also produce anabolic cytokines such as the bone morphogenetic protein family members and insulin-like growth factor-1 (IGF-1), which induce the synthesis of collagen and initiate the proliferation of chondrocytes [3]. A disruption of

* Correspondence: blue@hs.med.kyoto-u.ac.jp
[1]Department of Tissue Regeneration, Institute for Frontier Medical Sciences, Kyoto University, 53 Kawahara-cho, Shogoin, Sakyo-ku, Kyoto 606-8507, Japan
Full list of author information is available at the end of the article

the equilibrium between the catabolic and anabolic activities results in catastrophic damage to the articular cartilage, ultimately inducing the pathological condition known as OA.

Prostanoids, including prostaglandin (PG) D2, PGE1, PGE2, PGF2α, prostacyclin (PGI2), and thromboxane A2, are lipid mediators produced in a sequence of cyclooxygenase (COX) -1, -2-catalyzed reactions [8]. The role of PGE2 in the development of OA is controversial. Some reports point to an important role in inflammation [9]. Pro-inflammatory signaling mediators such as IL-1 and TNF-α induce the synthesis of PGE2 by promoting the expression or activities of COX-2 and microsomal PGE synthase-1 [10]. PGE2 then promotes IL-1 expression as part of a positive feedback mechanism, degrades the cartilage ECM [4,10-13], and finally induces apoptosis of chondrocytes [3]. Other reports insist that PGE2 opposes the effect of IL-1 [14] and stimulates the gene expression of type II collagen [3,15]. In addition, PGE2 stimulates the synthesis of proteoglycan and collagen through the expression of an IGF-1-binding protein [16,17]. PGE2 works through four isoforms of the EP receptor, EP1 to EP4. Previously, we considered that the controversy could result from differences in the mode of action and tissue distribution of each receptor [18]. Using an EP2 selective agonist, we showed that EP2 receptor-mediated PGE2 signaling enhances the growth of chondrocytes [18,19] and promotes the regeneration of articular cartilage in rabbits with cartilage defects [19].

In the current study, we investigate the effect of an EP2 agonist on articular cartilage in a rabbit model of traumatic degeneration.

Materials and methods

Materials

Microspheres loaded with a selective EP2 agonist, ONO-8815Ly (lysine salt) [20], were prepared by the emulsion-solvent evaporation method [19,21]. Briefly, ONO-8815Ly and polylactic-co-glycolic acid (PLGA) were mixed to form a water/oil emulsion, and added to the outer water phase containing polyvinyl alcohol under stirring with a turbine-shaped mixer at 5000 rpm to obtain a water/oil/water emulsion. PLGA microspheres that did not contain ONO-8815Ly in its free form were recovered by centrifugation and lyophilized to remove residual organic solvent and water. Then, a gelatin aqueous solution (20%, w/w) was poured into the microsphere suspension to form a gel. For the crosslink reaction, a glutaraldehyde aqueous solution (12.5 mg/ml) was poured into the microsphere suspension. Small cylinder-shaped gelatin hydrogels (4 mm in diameter and 2 mm in thickness) containing ONO-8815Ly (0, 80, or 400 μg of ONO-8815/gel) were obtained by hollowing out the gelatin hydrogel sheet. Diffusion kinetics analyses showed that ONO-8815Ly is gradually released from the microsphere over a period of seven days *in vitro* (Figure 1).

Animal model for traumatic degeneration

Four-month-old female Japanese white rabbits (weighing approximately 3 kg) were used. Traumatic degeneration was induced as described for the anterior cruciate ligament and menisectomy transection (ACLMT) model [22]. Operations were performed under general anesthesia, and a skin incision was made on the medial side of the patella. Soft tissues and articular capsules were cut to expose the knee joints. The anterior cruciate ligament was transected at the attachment to the tibia in the knee-flexed position, and the anterior horn of the medial meniscus was resected. The articular capsule and skin were sutured in layers with 4-0 nylon sutures. After the operation, rabbits were allowed to move freely. Preliminary experiments revealed that osteoarthritic changes were observed in this model at as early as two weeks after operation (data not shown).

Treatments with the EP2-agonist

A total of 64 animals were randomly assigned to five groups: G-S (sham operation), G-C (no further treatment), G-0, G-80, and G-400 (single intra-articular administration of gelatin hydrogel containing 0, 80, and 400 μg of ONO-8815Ly, respectively). Sham-operated rabbits (G-S; n = 4) received no further treatment, and were sacrificed either 2 (n = 2) or 12 weeks (n = 2) after the operation.

The ACLMT surgery was performed on both the knees of each of the remaining 60 rabbits to avoid any unequal bearing of weight due to pain on one side. No further treatment was performed in animals of the

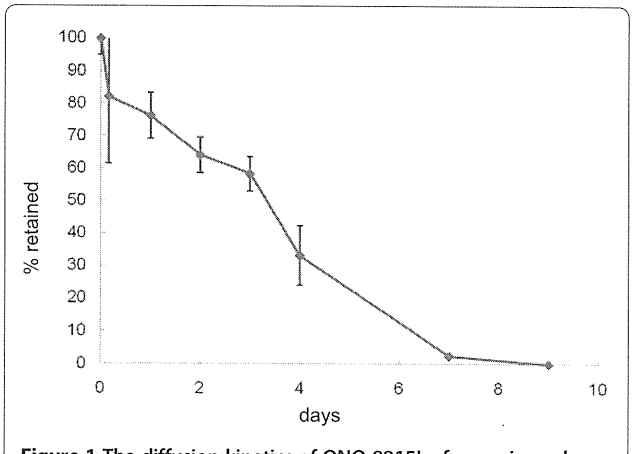

Figure 1 The diffusion kinetics of ONO-8815Ly from microspheres *in vitro*. Microspheres loading ONO-8815Ly were soaked in PBS, and the amount of retained ONO-8815Ly at each time point was measured by high-performance liquid chromatography and calculated as the ratio to the initial amount (n = 5).

control group (G-C; n = 12). In the treatment groups, no further treatment was performed on the right knee, but a gelatin hydrogel cylinder containing ONO-8815Ly (G-0, G-80, and G-400; n = 16 per group) was placed on the fatty pad of the left knee at the time of operation. Rabbits were sacrificed two weeks (G-C, n = 6; G-0, G-80, and G-400, n = 10 per group) or 12 weeks (n = 6 per group) after the operation. All the experiments with animals were approved by the institutional animal research committee, and performed according to the Guidelines for Animal Experiments of Kyoto University.

Histological examination

Rabbits were sacrificed 2 or 12 weeks after surgery, and the distal femur and proximal tibia of the left side of each animal were resected, fixed at 4°C overnight in a 10% formalin solution, and decalcified in formic acid for three days. After neutralization by 10% sodium sulfate for 24 hours, the samples were embedded in paraffin. Serial sections were prepared in the coronal plane through the middle of the femoral and tibia condyles, and one section from each sample was used for each of the histological analyses. In every section, the entire cartilage portion in full depth was evaluated. The specimens were stained with safranin O/Fast Green or H&E using standard procedures. The histological grade of cartilage degeneration was evaluated using the modified Mankin's scoring system [23], which was adopted as the original system [24] for the evaluation of the rabbit model. All the results shown herein represent the combined scoring data of two researchers.

Immunohistochemical analyses

Immunohistochemical examination was performed as follows. In brief, after deparaffinization, sections were incubated with 0.3% hydrogen peroxide for 30 minutes. Then, sections were treated with proteinase K for two minutes (proliferating cell nuclear antigen [PCNA] staining) or with hyaluronidase for 60 minutes (MMP staining), after which they were incubated with the following primary antibodies: mouse anti-human PCNA monoclonal antibody (1:100; Dako, Glostrup, Denmark), mouse anti-human MMP-13 monoclonal antibody (1:20; AnaSpec Inc., San Jose, CA, USA), or mouse anti-rabbit MMP-3 monoclonal antibody (1:50; Daiichi Fine Chemical Co. Toyama, Japan). All antibody dilutions were made in PBS. After an overnight reaction with the primary antibody at 4°C, sections were incubated with horseradish peroxidase-conjugated anti- mouse IgG (Vector Laboratories, Southfield, MI, USA) at room temperature for 30 minutes. Signals were visualized with 3, 3'-diaminobenzidine tetrahydrochloride, and nuclei were counterstained with hematoxylin. The percentage of PCNA-, MMP-13-, and MMP-3-positive cells in the cartilage was calculated by methods similar to those described above. Results of histological and immunohistochemical analyses were evaluated by two observers who were blinded to the identity of each sample.

Primary chondrocyte cultures

Primary culture of chondrocytes was performed using articular cartilage tissues harvested from non-treated rabbits (NRC cells) or ACLMT-operated rabbits (ORC cells). Briefly, thinly sliced cartilage tissues were incubated with collagenase (4 mg/ml; Sigma Aldrich, St. Louis, MO, USA) in DMEM for 12 hours. Cells were then collected by centrifugation, seeded into type I collagen-coated dish (Corning International K.K.,Tokyo, Japan), and cultured with DMEM containing 10% FBS supplemented with 100 units/ml penicillin and 100 mg/ml streptomycin at 37°C in a humidified atmosphere of 5% CO_2/95% air. Chondrocytes were grown in monolayer cultures, and were passaged when reaching confluence. Cells at the second passage were used for the assay. ONO-AE1-259-01, a selective agonist of EP2, was used to stimulate EP2 signaling in the presence or absence of IL-1β (Sigma Aldrich, St. Louis, MO, USA).

Real-time PCR

Total RNA was extracted from cultured cells using the RNeasy kit (Qiagen, Valencia, CA, USA) according to the manufacturer's protocol. All reverse transcription reactions were performed with an RT-PCR kit using 1 μg of total RNA with a Superscript II reverse transcriptase (Invitrogen, Carlsbad, CA, USA) for conversion into cDNA. The mRNA expression levels of *MMP-13* and glyceraldehyde 3-phosphate dehydrogenase (*GAPDH*) were quantified by real-time PCR using SYBR Green (Applied Biosystems, Foster City, CA, USA) and the ABI 7500 Real-Time PCR System (Applied Biosystems, Foster City, CA, USA). All reactions were run in triplicate, and the amount of PCR product of each gene was calculated using the standard curve method and normalized to *GAPDH* levels, which were used as an internal control. Using the ratio obtained for the untreated sample as a standard (1.0), the relative ratio of the treated samples was presented as the relative expression levels of the *MMP-13* gene. Sequences of primers used in this experiment were as follows: 5'-aggagcatggcgacttctac-3' and 5'-taaaacagctccgcatcaa-3' (*MMP-13*) and 5'-gctctccagaacatcactcctgcc-3' and 5'-cgttgtcataccaggaaatgagct-3' (*GAPDH*).

Statistical analysis

The statistical analyses were performed using the Statcel2 software (The publisher OMS Ltd., Saitama, Japan). The results are shown as the mean ± standard deviation (SD). The Kruskal-Wallis test was performed for screening

purposes, and the Steel-Dwass method for multiple comparisons was used if there was a significant difference between samples. A P value less than 0.05 was considered to be significant.

Results

Therapeutic effect of ONO-8815Ly in the early stages of degeneration

At two weeks after the operation, articular cartilages in medial condyles of G-C (Figure 2a, b) and G-0 (Figure 2a, c) showed severe degenerative findings such as surface irregularity including clefts and reactive changes such as clonal proliferation of chondrocytes. The intensity of safranin O staining was reduced in G-C (Figure 2a, g) and G-0 (Figure 2a, h). The grade of degenerative findings was less prominent in sections of G-S (Figure 2a, a), G-80 (Figure 2a, d) and G-400 (Figure 2a, e) than in those of G-C or G-0. Safranin O staining was stronger in sections of G-80 (Figure 2a, i) and G-400 (Figure 2a, j). Similar findings were observed in sections prepared from lateral femoral condyles. The degenerative changes were less prominent and the safranin O staining was stronger in sections of G-S (Figure 2b a and 2f), G-80 (Figure 2b, d and 2i) and G-400 (Figure 2b, e and 2j) than in those of G-C (Figure 2b, b and 2g) or G-0 (Figure 2b, c and 2h).

Histological grade was evaluated using a modified Mankin's scoring system [23,24]. The grades of medial condyle in each sample were scored and mean values were compared (Figure 2c). Scores were significantly better for G-80 than for G-0. The effect of ONO-8815Ly was more prominent in lateral condyles, and both G-80 and G-400 showed much better scores than G-C or G-0 (Figure 2d).

Similar findings were observed in medial (Figure 3a) and lateral (Figure 3b) condyles of tibiae. The degenerative changes were less prominent and the safranin O staining was stronger in sections of ONO-8815Ly-treated groups (G-80 and G-400) than in those of non-treated groups (G-C and G-0). The effect of ONO-8815Ly was similar between G-0 and G-80 in medial condyles (Figure 3c), whereas G-80 and G-400 showed better values than G-C or G-0 in lateral condyles (Figure 3d). These results suggested that ONO-8815Ly prevents degenerative change in articular cartilages during the early stages.

Therapeutic effect of ONO-8815Ly in the late stages of degeneration

Similar analyses were performed using sections prepared at 12 weeks after surgery. In the case of femoral condyles, no improvements of cartilage degeneration were observed in sections of ONO-8815Ly-treated groups (G-80 or G-400) (Figure 4a, d and 4e) and the staining of safranin O also showed no difference (Figure 4a, i and 4j). Similar results were obtained in lateral condyles of femora (Figure 4b). In agreement, there was no significant difference in Mankin's score in the analyses of medial (Figure 4c) or lateral (Figure 4d) condyles of femora.

Similar results were obtained in the tibiae. Neither medial nor lateral condyles showed better histological features by the treatment with ONO-8815Ly, and the Mankin's score showed no improvements (data not shown).

These results suggested that the effect of ONO-8815Ly failed to last, at least when using this drug delivery system.

Growth promoting effect of ONO-8815Ly

The proliferating activity of chondrocytes was evaluated by PCNA staining (Figure 5). The proportion of PCNA-positive cells in femoral (Figures 5a and 5b) and in tibial (Figures 5c and 5d) condyles at two weeks after operation were similar among all groups, suggesting that the improvement of cartilage degeneration by the EP2 agonist was not due to the acceleration of cell proliferation.

EP2- selective agonist inhibits the expression of MMP-13 in ACLMT

MMP-3 and MMP-13 are major proteases degrading the ECM. The expression of these enzymes was analyzed by immunohistochemistry using samples prepared at two weeks after the operation. For MMP-3, there were no significant differences in staining intensity or number of positive cells between any of the groups (Figure 6). For MMP-13, however, significant differences were observed (Figure 7). The staining of MMP-13 was much stronger in G-C and G-0 (Figure 7a, b and 7c) than in G-S, G-80, or G-400 (Figure 7a, a, d, and 7e). The proportion of MMP-13-positive cells was significantly lower in sections of G-80 and G-400 than in sections of G-C or G-0 (Figure 7b). Similar results were obtained for the intensity (Figure 7a, f, i, and 7j) and the ratio of MMP-13-positive cells (Figure 7c) in the analyses of lateral condyles.

EP2-selective agonist inhibits IL-1β-induced *MMP-13* mRNA expression

To confirm the effect of EP2 agonist on MMP-13 expression, the expression of the *MMP-13* gene by primary cultured chondrocytes was evaluated by quantitative real-time PCR (Figure 8). The expression levels of *MMP-13* were similar in NRC and ORC cells under basal culture conditions. Similarly, EP2 agonist treatment showed no significant effects on *MMP-13* levels on either cells. When NRC and ORC cells were treated with IL-1β (50 pg/ml), the expression levels of *MMP-13* mRNA were significantly increased in both cells. IL-1β-induced expression of MMP-13 mRNA in ORC cells was reduced by

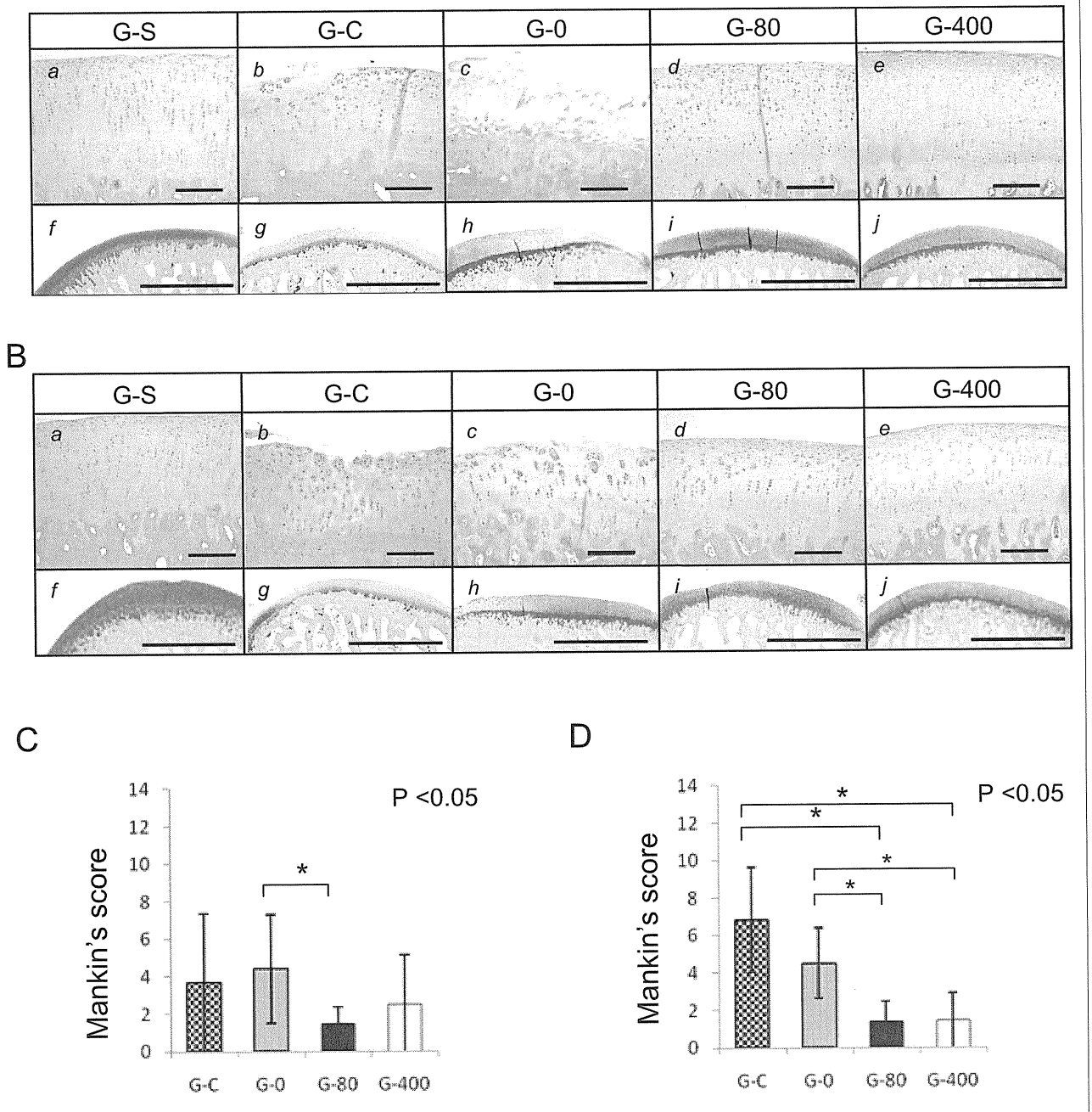

Figure 2 Effect of ONO-8815Ly in the early stages of OA (femur). Histological findings and grade of degeneration, scored using Mankin's system, in (**a**) medial and (**b**) lateral femoral condyles at two weeks after the operation. Sections were prepared from samples of (*a* and *f*) G-S, (*b* and *g*) G-C, (*c* and *h*) G-0, (*d* and *i*) G-80, and (*e* and *j*) G-400, and stained with (*a* to *e*) H&E or (*f* to *j*) safranin-O. Magnification, 200× (H&E) and 40× (safranin-O). Scale bar, 200 μm (HE) and 2.0 mm (safranin-O). *$P < 0.05$. Values are the mean ± standard deviation. OA, osteoarthritis.

co-treatment with the EP2 agonist in a dose-dependent manner, and the maximum reduction was 37% at 1 μM of EP2 agonist. In the case of NRC cells, the maximum reduction (27%) was observed at the concentration of 0.1 μM.

Discussion

The effect of PGE2 on the progression of OA is still a matter of debate. In some reports, PGE2 was shown to destroy articular cartilage by degrading cartilage ECM [12,13]. It has also been reported to down-regulate the

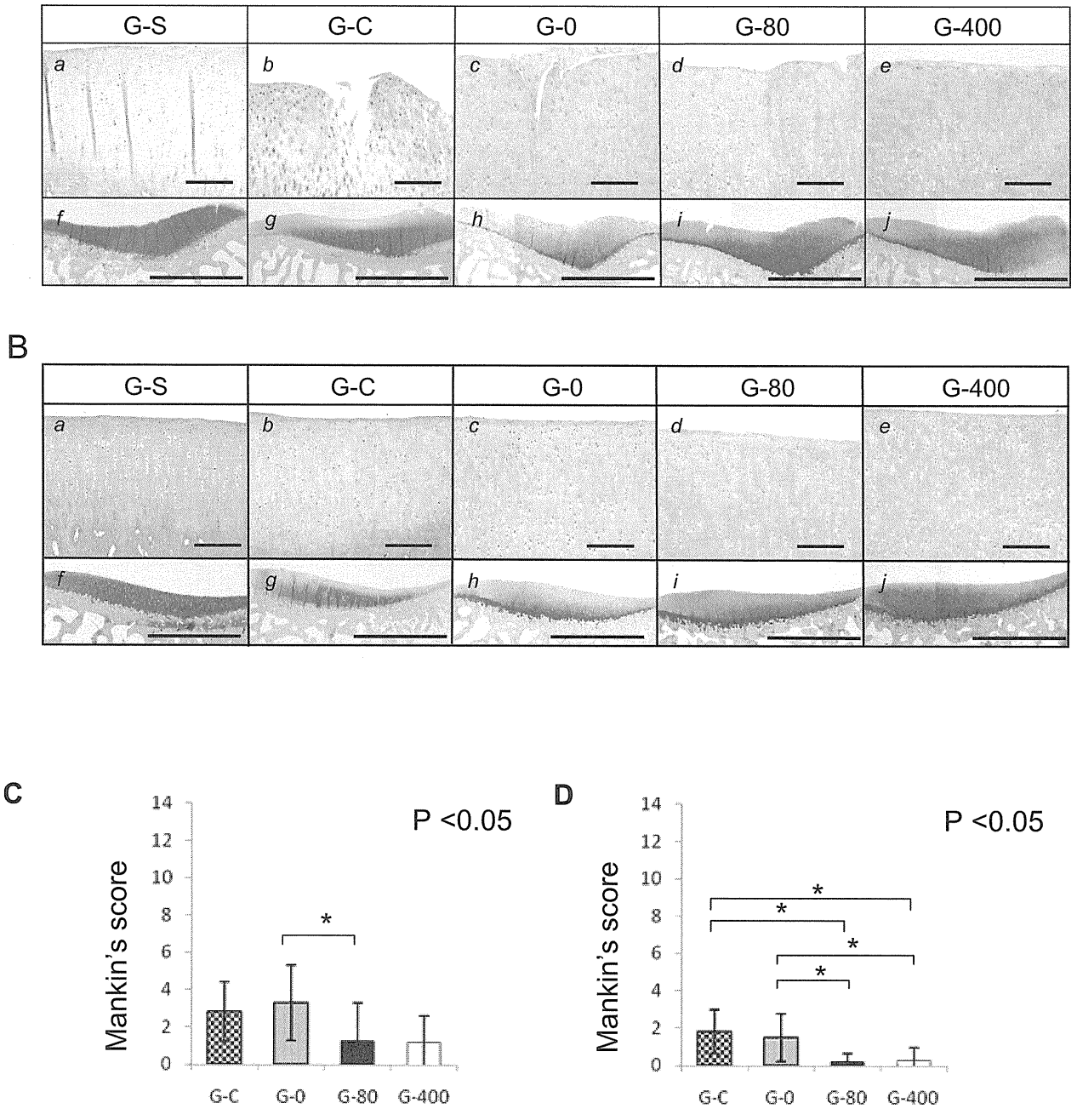

Figure 3 Effect of ONO-8815Ly in the early stages of OA (tibia). Histological findings and grade of degeneration, scored using Mankin's system, in (**a**) medial and (**b**) lateral tibial condyles at two weeks after the operation. Sections were prepared from samples of (*a* and *f*) G-S, (*b* and *g*) G-C, (*c* and *h*) G-0, (*d* and *i*) G-80, and (*e* and *j*) G-400, and stained with (*a* to *e*) H&E or (*f* to *j*) safranin-O. Magnification, 200× (H&E) and 40× (safranin-O). Scale bar, 200 μm (H&E) and 2.0 mm (safranin-O). *$P < 0.05$. Values are the mean ± standard deviation. OA, osteoarthritis.

production of IL-6 by IL-1α and IL-1β via EP2/EP4 receptors [25,26]. PGE2 at very low concentrations inhibits the production of IL-1β, TNF-α, and MMP-13 in the articular cartilages of OA patients [27]. In the current study, the production of MMP-13 was decreased by an EP2 agonist (Figures 7 and 8), which is consistent with the *in vitro* data described in a recent report [28]. Continuous administration of non-steroidal anti-inflammatory drugs to patients with OA exacerbates OA [29,30]. These contradictory results

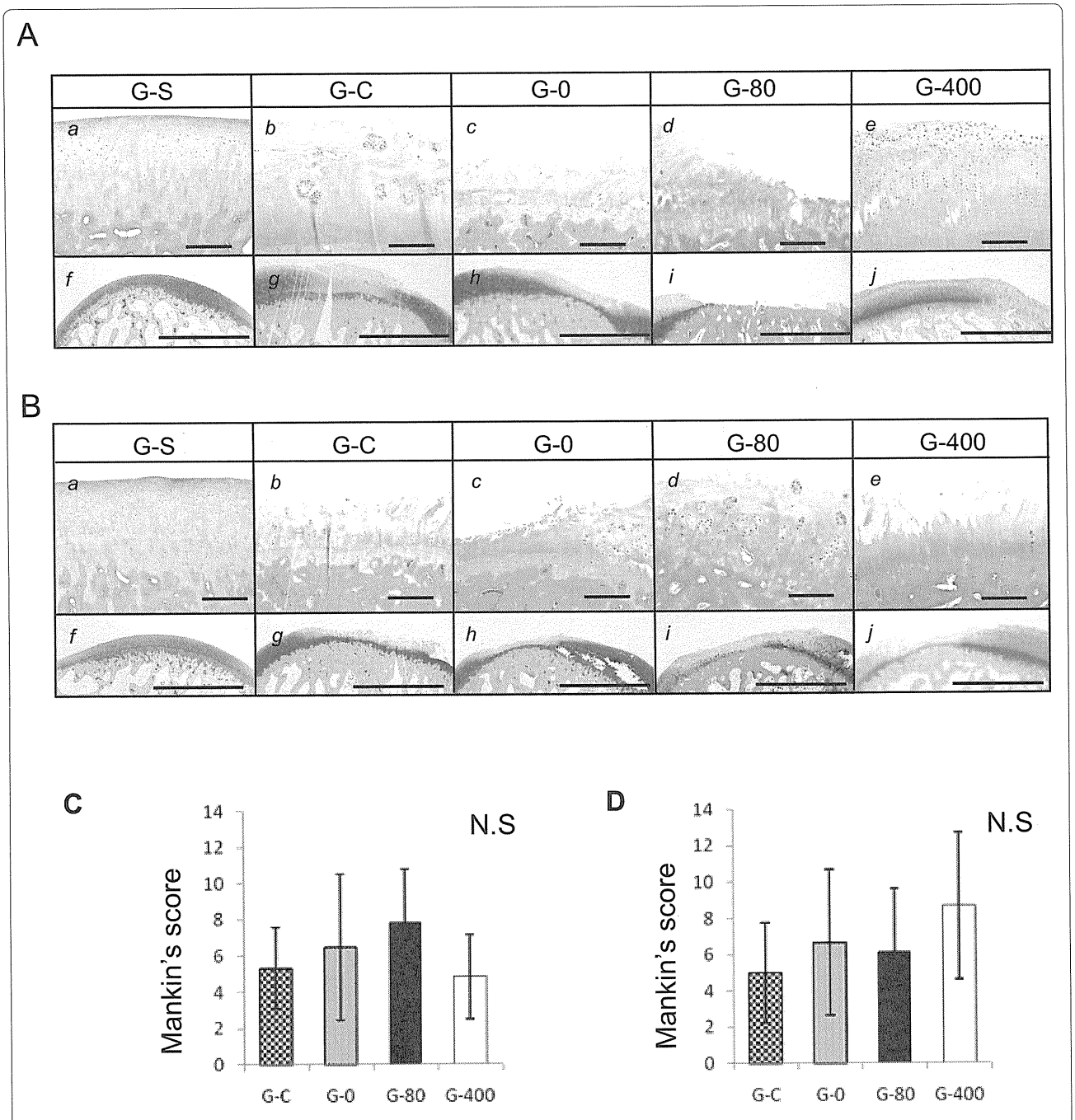

Figure 4 Effect of ONO-8815Ly in the late stages of degeneration (femur). Histological findings of **(a)** medial and **(b)** lateral femoral condyles at 12 weeks after the operation. Sections were prepared from samples of (*a* and *f*) G-S, (*b* and *g*) G-C, (*c* and *h*) G-0, (*d* and *i*) G-80, and (*e* and *j*) G-400, and stained with (*a* to *e*) H&E or (*f* to *j*) safranin-O. Magnification, 200× (H&E) and 40× (safranin-O). Scale bar, 200 μm (H&E) and 2.0 mm (safranin-O). Grade of degeneration scored using Mankin's system in **(c)** medial and **(d)** lateral femoral condyles at 12 weeks after the operation. Values are the mean ± standard deviation. N.S, not significant.

may be due to the differences in the experimental dose of PGE2 agonist used, or due to the pleiotropic effects of PGE2 through different types of receptors (EP1 to EP4). Therefore, analyses should be conducted with agonists specific for each type of receptor. IL-1β-induced expression of *MMP-13* mRNA was reduced by EP2 signaling both in NRC and ORC cells *in vitro* (Figure 8). Moreover, IL-1β-induced expression of *MMP-13* mRNA was reduced in ORC cells, but not in NRC cells, in a dose-dependent manner, that is, *MMP-*

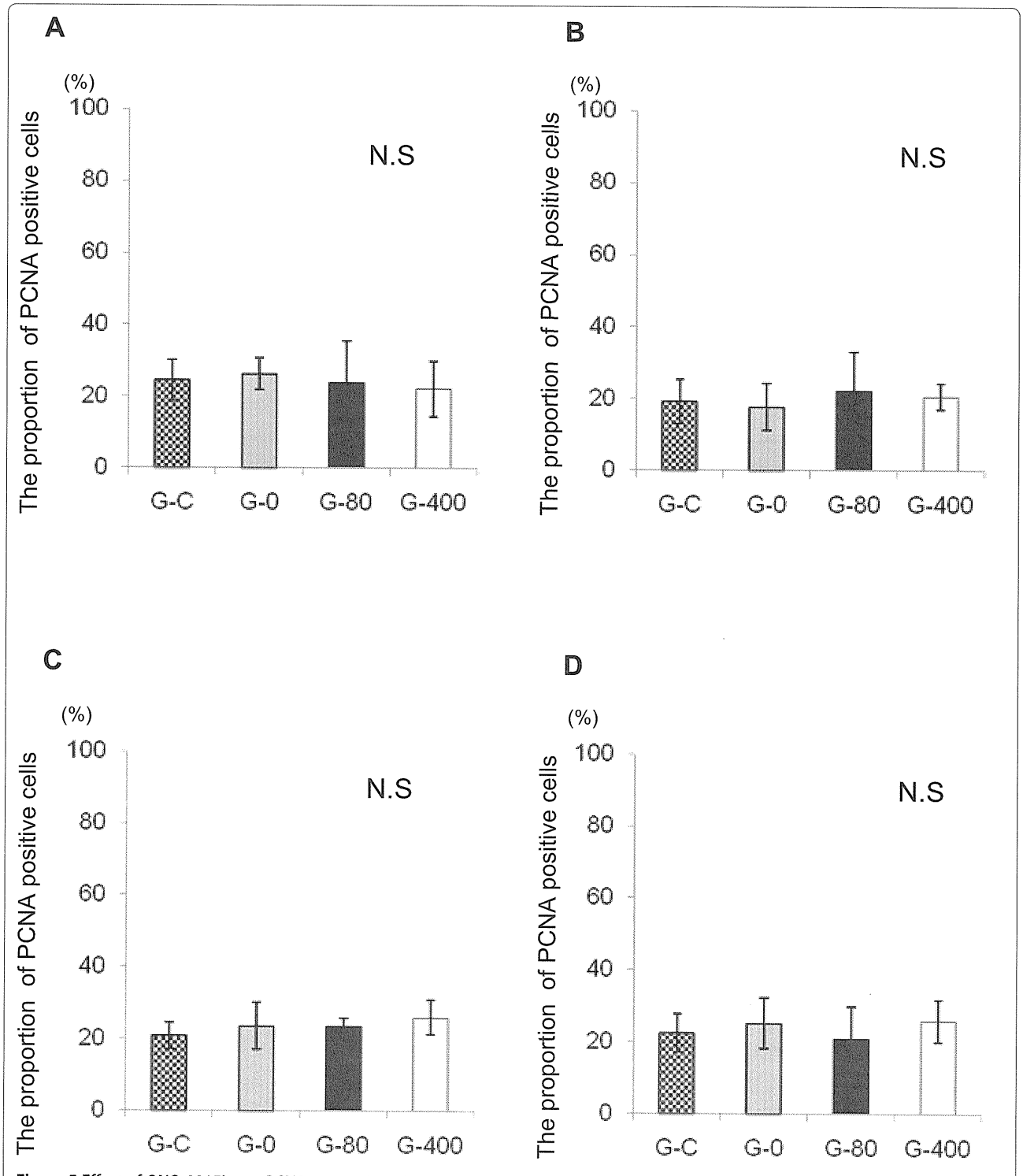

Figure 5 Effect of ONO-8815Ly on PCNA expression. The proportion of PCNA-positive cells in **(a)** medial and **(b)** lateral femoral condyles, and in **(c)** medial and **(d)** lateral tibial condyles. Values are the mean ± standard deviation. N.S, not significant; PCNA, proliferating cell nuclear antigen.

13 expression was higher in the presence of 1 μM of ONO-AE-259-01 than in the presence of 0.1 μM of ONO-AE-259-01 (Figure 8). An EP2 agonist acts as an anti-inflammatory drug at low doses, but if the concentration exceeds 1 μM, the anti-inflammatory effect may become weak (Figure 8). In fact, some authors have reported that excess EP2 agonists may act rather as inflammatory-inductive drugs.

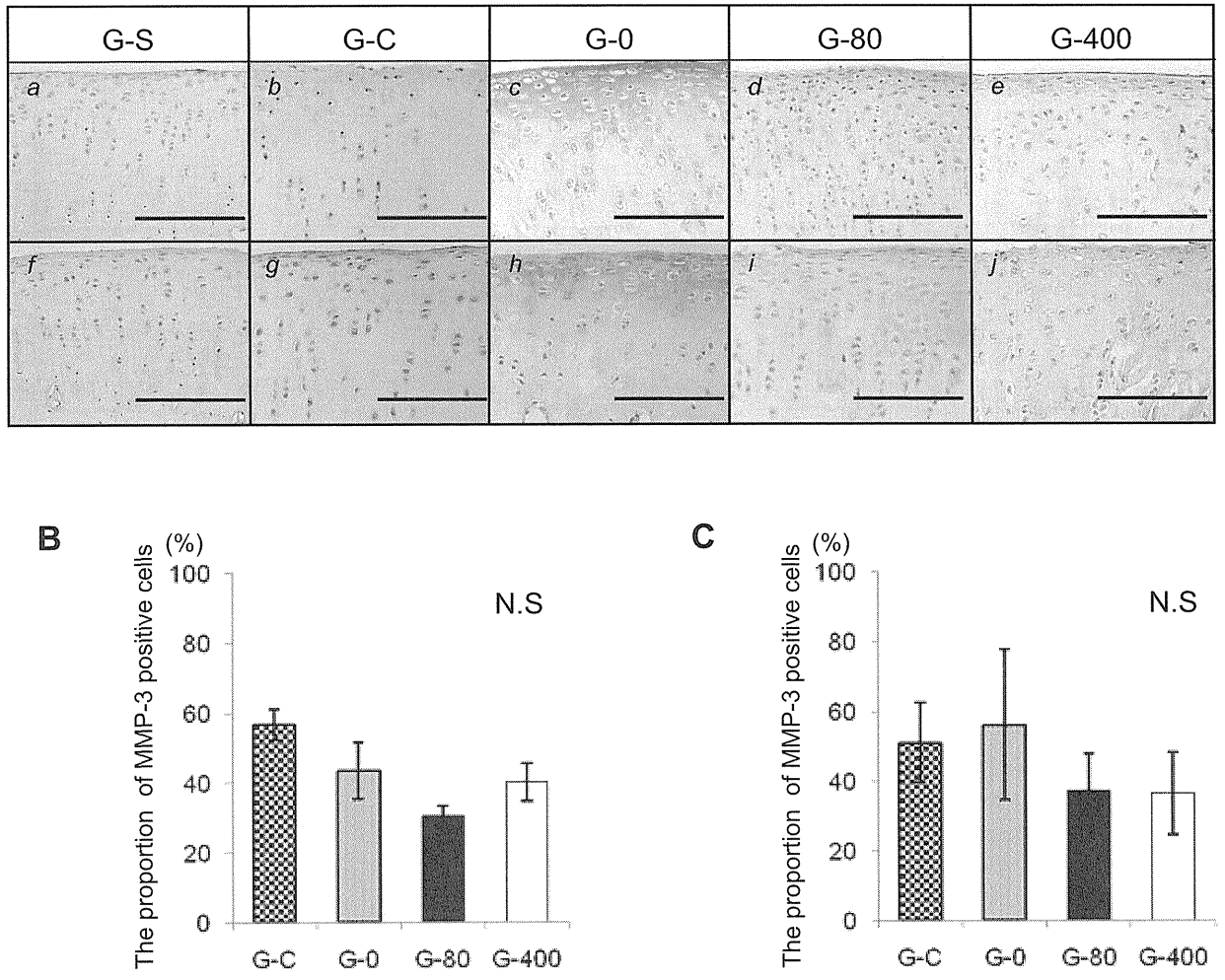

Figure 6 Effect of ONO-8815Ly on the expression of MMP-3 in femoral condyles. **(a)** Immunostaining for MMP-3 at two weeks after the operation. Sections of (*a* to *e*) medial and (*f* to *j*) lateral femoral condyles were prepared from samples of (*a* and *f*) G-S, (*b* and *g*) G-C, (*c* and *h*) G-0, (*d* and *i*) G-80, and (*e* and *j*) G-400. Magnification, 400×. Scale bar, 200 μm. Proportion of MMP-3-positive cells in **(b)** medial and **(c)** lateral femoral condyles at two weeks after the operation. Values are the mean ± standard deviation. *$P < 0.05$. MMP-3, matrix metalloproteinase-3; N.S, not significant.

Previously, we showed that EP2 signaling enhances the growth of chondrocytes [18,19] and promotes the regeneration of articular cartilage in rabbits with cartilage defects by an EP2-selective agonist [19]. However, in the current study, EP2 signaling failed to promote chondrocyte proliferation (Figure 5). The differences may result from differences in the animal models. In the previous study, the effect of EP2 signaling on articular cartilage was evaluated using the chondral and osteochondral defect models. In that model, cartilage defects are present before initiation of the treatment with an EP2 agonist. Thus, EP2 signaling may promote cartilage regeneration by inducing proliferation of cartilage chondrocytes and, consequently, contributing to ECM reconstruction. On the other hand, in the present study, the articular chondrocytes appeared normal immediately after the ACLMT operation, and EP2 signaling reduced cartilage degeneration caused by traumatic instability of the knee joint. These differences in models might be the cause of difference in the results.

In the present study, the abnormal stress on cartilage tissues induced by joint instability was the main cause of degeneration. The degeneration was more remarkable in the lateral (Figures 2d and 3d) than in the medial components (Figures 2c and 3c), wherein partial meniscectomy was performed. We have no clear explanation for this